Russian Chemical Reviews **79** (12) 1047 – 1070 (2010) © 2010 Russian Academy of Sciences and Turpion Ltd

DOI 10.1070/RC2010v079n12ABEH004167

Kinetics of fast photochemical charge separation and charge recombination reactions

A I Ivanov, V A Mikhailova

Contents

I.	Introduction	1047
II.	Mechanisms of fast photoinduced charge transfer reactions	1048
III.	The free energy gap law	1049
IV.	Nonequilibrium effects in the ultrafast charge transfer reactions	1052
V.	The spectral effect	1061
VI.	Conclusion	1067

Abstract. The review is devoted to studies of the kinetics of fast photochemical processes in liquid solutions. With use of abundant experimental data and results of theoretical simulations, it is shown that a nonequilibrium state of the nuclear subsystem plays a key role in ultrafast charge transfer processes. A comparison of different approaches and theories developed in recent years for a quantitative description of fast chemical processes is performed and influence of spectral characteristics of an exciting pulse, as well as that of dynamic properties of solvents on the kinetics of these processes are analyzed. The methods to control the efficiency of photochemical charge transfer reactions in a nonequilibrium mode are systematized. The bibliography includes 187 references.

I. Introduction

Despite the fact that electron transfer (ET) is considered as the simplest process, the interest in its study has increased in the last few decades. It is determined by the following reasons. Firstly, ET underlies a huge number of processes occurring in animate and inanimate nature. Oxidation – reduction reactions, enzymatic conversions (primarily related to the energetics of living cells), electrochemical and, of course, physical processes [1–9] include ET as a key elementary step. It is necessary to emphasize that new processes of potential practical applicability, which include the ET stage, are continually appearing.[10, 11] Therefore further progress should be expected in this field of research in the coming years. For instance, ET in various donor – acceptor (DA) systems was studied in the past ten years for the purpose of their use in the form of thin films for transformation of the solar energy to the electricity. Such DA structures are perspective for construction of photovoltaic devices and also of chemical and biochemical sensors.[12]

Secondly, in spite of seeming simplicity of ET its mechanisms turned out utterly diverse. This is testified, for example, by the fact that rates of ET lie within a wide range (from micro- to femtoseconds). Obviously, the mechanisms of ET must be completely different for ultraslow and ultrafast processes. If the condition of thermodynamic equilibrium of the nuclear subsystem can be a good approximation for slow reactions, nonequilibrium effects are highly important for ultrafast reactions. Thus, nonequilibrium of the nuclear subsystem has to play a key role in reactions occurring in time shorter than the relaxation time of a medium.

Thirdly, some studies of the ET dynamics with femtosecond temporal resolution emerged quite recently, which allowed examination of this elementary act in details. Clearly, new physical ideas and conceptions are necessary for correct treatment of the results of these investigations. Consideration of ultrafast processes occurring under conditions of strong nonequilibrium of the nuclear subsystem is beyond the scope of chemical kinetics. Instead, methods of chemical dynamics based on quantum statistics have to be used.

Fourthly, studies of ET reactions belong to the field of chemistry, in which interplay of experiment and theory is especially productive, and this fact is powerful impetus of their progress. Notwithstanding increasing capabilities of experimental approaches and progress in quantum chemical theories, the major problem of ultrafast photochemical reactions of ET, viz. the control of their rates and quantum yields of their products, remains urgent.[13–15] Classification of available facts and theoretical approaches allows one to reveal the most important tendencies in development of the theory of ultrafast photochemical processes and predict the most probable achievements in the coming years.

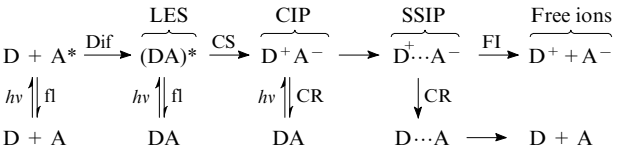
A I Ivanov, V A Mikhailova Volgograd State University, Universitetsky prosp. 100, 400062 Volgograd, Russian Federation. Fax (7-844) 246 02 79, tel. (7-844) 246 08 12, e-mail: Anatoly.Ivanov@volsu.ru (A I Ivanov), mixailova_va@mail.ru (V A Mikhailova)

Received 21 June 2010
Uspekhi Khimii **79** (12) 1137 – 1163 (2010); translated by S E Boganov

II. Mechanisms of fast photoinduced charge transfer reactions

From the standpoint of classical kinetics ET is an elementary chemical act, and there is no point to discuss its mechanism. However investigation of ET revealed many detailsthe the analysis of which forced to divide this act into several processes and stages. The set of these processes is naturally called the mechanism of the elementary act of ET. Quite general scheme of photoinduced reactions of ET in polar media which includes majority of the stages under discussion at present can be shown as follows:

Scheme 1



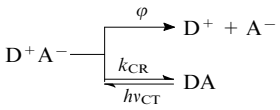
Here the index *hv* denotes the stage of photoexcitation of reactants leading to a locally excited state of the DA pair or to the direct formation of a charge transfer complex D^+A^-; fl means fluorescence. Scheme 1 shows the majority of possible processes, intermediate states and interconversions among them: diffusion (Dif), charge recombination (CR), charge separation (CS), locally excited state (LES) of DA complexes $(DA)^*$, contact ion pair (CIP) or tight (intimate) ion pair (TIP), solvent-separated ion pair $D^+\cdots A^-$ (SSIP) or loose ion pair (LIP), free ions $D^+ + A^-$ (FI) which the solvent-separated ion pair decays to. It is worth noting that the detailed information of the structure of intermediate species such as the contact and solvent-separated ion pairs is usually derived from indirect evidences. By this reason the structures of such pairs are poorly examined, nevertheless it is known for certain that the structures largely depend on the means of formation of the pairs.

In the contact ion pair ions are tightly adjacent to each other, so there is neither solvent molecule nor any other neutral molecule between them. This is their major distinction from SSIP or LIP, in which the ions are separated by several solvent molecules or by other neutral molecules. Therefore the contact ion pairs are also called TIP. At present one can determine some characteristics of these ion pairs such as typical lifetimes by methods of optical spectroscopy of ultra-high time resolution, however strong broadening of the electron transition bands being usual for the liquid phases conceals the structural difference between the contact and free ion pairs. It is a reason that the exact microscopic structure of the intermediate ion pairs is not known till now. It is often supposed that the contact ion pairs formed by aromatic ions have a sandwich structure with a typical interionic distance of ca. 3.5 Å.[16] Sometimes the contact ion pairs fluoresce, indicating formation of exciplexes,[17–19] *i.e.* of contact ion pairs with incomplete ET. Such states represent superposition of locally excited states D^*A and DA^*, as well as of the charge transfer state D^+A^-, and have charge separation $\delta < 1$.[17–21] Relatively stable exciplexes $D^{\delta+}A^{\delta-}$ are formed in weakly polar and nonpolar media only.[20] As a rule, in polar media they dissociate fast into radical ions. Besides the fluorescence quantum yield in polar solvents is very low in most cases, which means that the emission rate constants are small as compared with the rate constants of the ion dissociation or recombination. Exciplexes are not shown in Scheme 1 as they do not play any appreciable role in the processes which will be discussed below.

Even less is known about the structure of the loose ion pairs. Among them the solvent-separated ion pairs are often singled out, which are considered either as species possessing defined geometry [16, 22, 23] and, hence, specific dissociation and recombination rate constants or as pairs of diffusing ions at distances, where their recombination is effectual. The interionic distances in the solvent-separated ion pairs vary from 7 to more than 12 Å.[16, 24–28]

In the simplest case when all intermediate states are excluded, the photoexcitation of the DA complexes in their charge transfer absorption band results in formation of contact radical-ion pairs in polar solvents. Further transformations of such pairs proceed in two competitive directions, which are recombination of a pair to its ground state (the CR stage) and formation of free ions (the FI stage). The ET process of this type can be represented by the following simpler scheme

Scheme 2



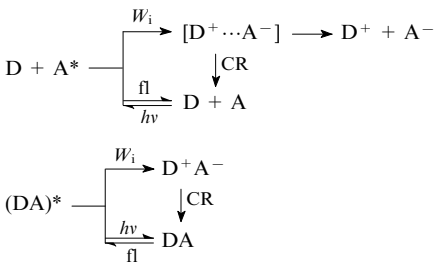
where ν_{CT} is the frequency of the maximum of the charge transfer absorption band, k_{CR} is the rate constant for the charge recombination stage (the CR stage), φ is the quantum yield of the free ions (the FI stage).

According to the experimental data,[29–37] the charge recombination in the excited DA complexes is usually ultrafast process and the quantum yield of the free ions is negligible. Therefore Scheme 2 represents the simplest process of charge separation the description of which can be restricted by consideration of two electronic states only. Those are the ground state of the DA complex $|1\rangle$ and the final charge transfer state $|2\rangle$. In accordance with elementary conceptions formulated by Mulliken,[38] the ground state has some ionic character with the charge separation equal to δ, whereas the final state has incomplete charge separation of the ionic degree $1 - \delta$.

Systematic studies of the kinetics of the complexes which were photoexcited at the frequency of charge transfer absorption band, demonstrated that the fast charge recombination occurs in nonequilibrium of nuclear subsystem and its regularities are ultimately different from those of the equilibrium recombination.[37, 39–42] Such reactions are called ultrafast reactions, emphasizing that their typical rates are higher than the rates of solvent relaxation.

The photoinduced reactions of inter- and intramolecular ET are usually rendered as follows:

Scheme 3



W_i is ionization rate.

In this case, a state without appreciable charge separation (a locally excited electronic state) is formed upon photoexcitation; therefore, the scheme should include three electronic states at least:

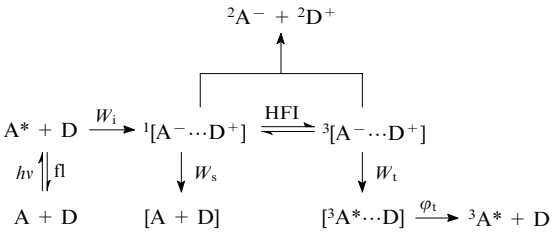
$|1\rangle$ — the ground state;

$|2\rangle$ — the locally excited state;

$|3\rangle$ — the state with separated charge.

Due to availability of different spin states for some radical-ions and possibility of multiplet transitions the scheme of the ET reactions can be more complicated. For instance, the following scheme should be used for description of the effect of external magnetic field on yield of free ions and acceptors in the triplet states:[43,44]

Scheme 4



Here the possibility of a transition of the geminal ion pair $^1[A^-\cdots D^+]$ into its triplet state $^3[A^-\cdots D^+]$, induced by hyperfine interaction, HFI, and following recombination to the acceptor triplet state $^3A^*$ with quantum yield φ_t are taken into account (W_i, W_s, W_t are the rates of the corresponding transitions).

III. The free energy gap law

Extensive experimental and theoretical research were undertaken to understand the processes specified by ET.[1,2,4,6] The experimental fact that stimulated the development of theory of ET in polar media consists in the following. In the course of study of the ET reaction between ions in a polar solvent it was found that its activation energy (E_a) increases with the decrease of the ion radius (R_a). However the reverse dependence is intuitively expected. Therefore the major goal of the required ET theory was to explain how the energy barrier depends on the radius (R_a) and the nature of the ion. An idea that the potential barrier separating the starting and the final states in the ET process is caused by polarization of solvent was suggested first by Lybbi,[45] and then it was successfully used by Marcus.[46–48]

As at least one of the partners is charged in bimolecular ET reactions and, therefore, solvated in polar media (*i.e.* surrounded by suitably oriented solvent molecules), the description of ET (and also of charge separation and recombination processes) requires taking into account orientational alteration of surrounding molecules and reorganization of the medium around the charged species. Using classical macroscopic description of solvents (the continual model with the macroscopic specific orientation polarization), Marcus[46] was able to calculate the activation energy of the ET reaction in the polar solvent, linking it with the energy of solvent reorganization. Later on, strict quantum mechanical calculations of rate constants were carried out not only for the ET reactions in the polar solvents,[49–51] but also for electrochemical reactions of ET in metals, semiconductors and thin semiconductor films, as well as for a proton transfer reaction.[1] Besides, further theoretical studies revealed a universal relation of the rate constants of non-adiabatic ET reactions to an experimentally measurable quantity, *viz.* to the complex permittivity of media $\varepsilon(\omega)$ (Ref. 52), thereby ascertaining the role of dynamic characteristics of solvents in the kinetics of ET.

Further studies showed that reorganization of the polar solvent always has very important contribution (and, often, the main contribution) to the activation energy of the ET reactions; however, this is not the only factor. Intramolecular reorganizations of the donor and the acceptor are also critical. Significance of the effect of intramolecular vibrations [both classical low-frequency and high-frequency (HF) quantum vibrations] of the donor and the acceptor on the dynamics of the elementary act of ET was revealed in quantum mechanical computations of the probability of ET, carried out taking into account the changes in intramolecular states of the reactants and experimental data on kinetics of photoinduced ET obtained during the last 20 years.[1,4,39,53–56] Initially the importance of reorganization of the HF modes was recognized for highly exothermic reactions.[39,56] Particularly, it was shown that the principal effect of the quantum HF modes consists in lowering of the activation energy and, therefore, increase of the reaction rate.[1,4,55,56] Later it was found that the reorganization of intramolecular HF vibrations can cause multiple acceleration of weakly exothermic reactions of ET, if these processes are nonequilibrium.[56,57]

In the 1970s the theory of the thermal ET reactions and charge redistribution was generalized to photoinduced processes.[58] According to existent terminology, ET reactions are called photoinduced, if at least one of the involved reactants is in its electronically excited state.

Returning to Marcus theory it is worth to emphasize that Marcus succeeded in adequate evaluation of the nonequilibrium orientation polarization of solvent upon the activation energy computation and demonstrated that the only solvent property affecting the reaction kinetics is its reorganization energy (E_{rm}), related to the activation energy by a simple equation

$$E_a = \frac{(\Delta G + E_{rm})^2}{4 E_{rm}}, \tag{1}$$

where ΔG is free Gibbs energy of the reaction. The energy of solvent reorganization in approximation of non-overlapping spheres can be approximately calculated from the formula[46]

$$E_{rm} = \frac{c_P e^2}{2}\left(\frac{1}{R_a} + \frac{1}{R_d} - \frac{2}{R_{ad}}\right). \tag{2}$$

Here

$$c_P = \frac{1}{\varepsilon_\infty} - \frac{1}{\varepsilon_0}$$

is Pekar's factor determined by optical (ε_∞) and static (ε_0) dielectric constants of the medium; e is the charge transferred in the reaction; R_a and R_d are the radii of the acceptor and the donor; R_{ad} is the distance between their centres.

In the framework of the microscopic quantum mechanical theory[1,4,55] the rate constant for the elementary chemical act of ET (k_{et}) depends not only on the distance between the donor and the acceptor ($r = R_{ad}$), but also on several other parameters determined by the energy pattern of the

elementary act of ET. The parameters of primary importance are the following: electronic matrix element for radiationless transition (V_{el}), energies of the reorganization of the solvent (E_{rm}) and the intramolecular vibrational modes (E_{rv}), and exothermicity of the reaction ($-\Delta G$). In the simplest two-level approximation (in which only the initial neutral and the final ET state are considered) without account of intramolecular mode reorganization the ET rate can be expressed by the following equation:

$$k_{et} = k_0(r, V_{el}) \exp\left[-\frac{(\Delta G + E_{rm})^2}{4 E_{rm} k_B T}\right], \quad (3)$$

where k_B is Boltzmann constant, T is the temperature. This well-known Marcus formula [46] is called the free energy gap law, because it defines quite narrow region for the reaction exothermicity appropriate for the ET reactions. Figure 1 illustrates this law, which determines a parabola (dashed line) in the plane ($\ln k_{et}, -\Delta G$).

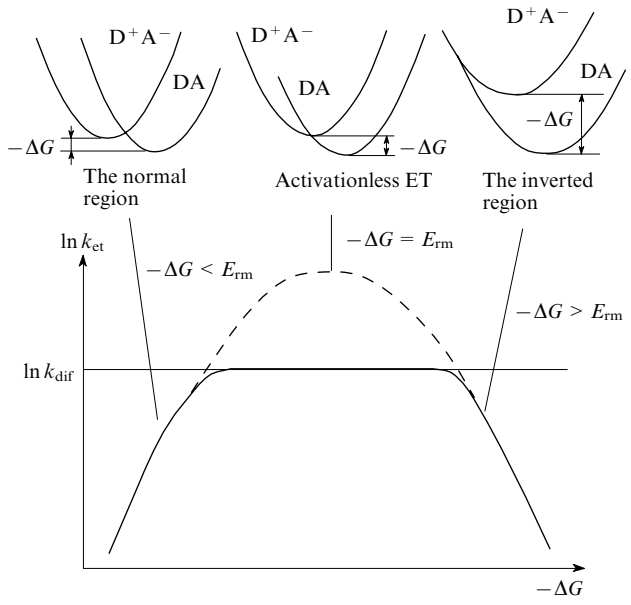


Figure 1. A scheme illustrating the free energy gap law and its interpretation.

When the distance between the donor and the acceptor is large the coefficient $k_0(r, V_{el})$ can be found in the framework of the perturbation theory using V_{el} expansion.[1] Therefore, as it follows from Eqn 3, the free energy gap law predicts quadratic dependence of $\ln k_{et}$ on the reaction free energy. This determines untypical behaviour of the ET reaction rate constant with increase of $-\Delta G$. According to the classification of Marcus,[46,47] the reaction of ET is 'normal' until $-\Delta G < E_{rm}$. In this region the rate of ET increases with increasing $-\Delta G$ (see Fig. 1) and reaches the maximal magnitude for activationless ET. However there is another so-called 'inverted' region, where paradoxic increase of the activation energy together with decrease of the reaction rate should be observed on going to energetically more favourable processes in accordance with Marcus law. Note that the terms 'normal' and 'inverted' regions are used to designate the direct (in the normal region with increase of the rate) and reverse (in the inverted region with decrease of the rate) dependences of the ET rates on the exothermicity, as well as to denote the exothermicity intervals ($-\Delta G < E_{rm}$) and ($-\Delta G > E_{rm}$), respectively.

By the time of the ascertainment of the free energy gap law, a paradigm of linear dependences on free energies, which was formulated in 1924 by Brønsted [59] on the basis of analysis of extensive experimental material, dominated in chemical kinetics. The Marcus free energy gap low contradicted the conception of monotonic variation of the rate of reaction depending on its exothermicity and was initially perceived with skepticism, as all available experimental data argued for existence of the normal region only in accordance with intuitive expectation. This skepticism was significantly corroborated by numerous results of studies of Weller and co-workers.[60–63] While studying the kinetics of fluorescence quenching owing to the charge transfer, which proceeds in accordance with the scheme

$$D^* + A \xrightarrow{CS} D^+\cdots A^- \xrightarrow{FI} D^+ + A^-, \quad (4)$$

they found that the rate constants of the quenching continuously increased with increase of exothermicity until getting the value typical for the diffusion control regime. They remain almost invariable even in the region of the highest exothermicity (Rhem — Weller's plateau). This result was in clear contradiction to Marcus law of the energy gap.

The first explanation of the existence of Rhem–Weller's plateau was suggested by Marcus and Siders.[64] They noticed that ET took place at a moment of diffusive approaching of reactants, therefore the observed rate constant for ET is expressed by the equation

$$k_i = \frac{k_c k_{dif}}{k_c + k_{dif}},$$

where k_c is the kinetic rate constant,

$$k_{dif} = 4\pi\sigma D$$

is the diffusion rate constant, σ is the sum of the contact radii of the reactants, D is the diffusion coefficient. If in the normal region $k_c \ll k_{dif}$, ET proceeds in the kinetic regime and $k_i \approx k_c$ reproduces the ascending branch of dependence of k_c in accordance with the free energy gap law. In the vicinity of the maximum the inequality $k_c \gg k_{dif}$ may be true and then $k_i \approx k_{dif}$ does not depend on ΔG giving the observed plateau. In accordance with this idea, Rhem–Weller's plateau is determined by the diffusion rate constant (see the lower part of the Fig. 1). However, this consideration does not explain why the inverted region is absent up to $\Delta G \approx -3$eV.

The other experimental fact contradicting with the free energy gap law consisted in monotonic decrease of the charge recombination rate with increase of the reaction exothermicity in DA complexes excited at the frequency of the charge transfer absorption band.[37,65] No normal region was observed in these experiments, instead, the rate constants for the charge recombination monotonously decreased with increase of the exothermicity in the whole range of accessible free energies of the reactions (from -0.5 to -3.0 eV).[29,66] Typical dependence $\ln k_{CR}(-\Delta G_{CR})$ is shown in Fig. 2.

Only in 1980s the parabolic law was supported in a series of experiments concerned predominantly with processes of intramolecular ET.[29,67–70] The results of the first system-

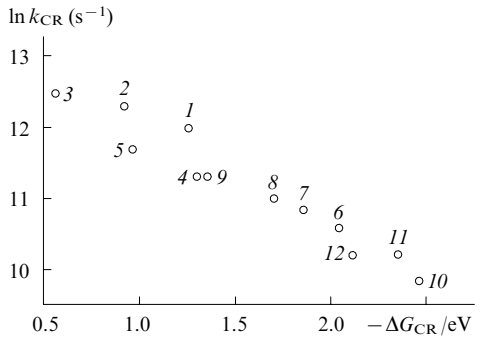


Figure 2. The dependence of the rate of charge recombination in the DA complexes on the reaction exothrmicity.[30]
(*1*) Naph–TCNE, (*2*) Pyr–TCNE, (*3*) Per–TCNE, (*4*) Naph–TCNQ, (*5*) Pyr–TCNQ, (*6*) Naph–PMDA, (*7*) Chr–PMDA, (*8*) Pyr–PMDA, (*9*) Per–PMDA, (*10*) Pyr–PA, (*11*) An–PA, (*12*) Per–PA.
Here: Naph is naphthalene, TCNE is tetracyanoethylene, Pyr is pyrene, Per is perylene, TCNQ is teracyanoquinodimethane, PMDA is pyromellite dianhydride, Chr is chrysene, PA is phthalic anhydride, An is anthracene.

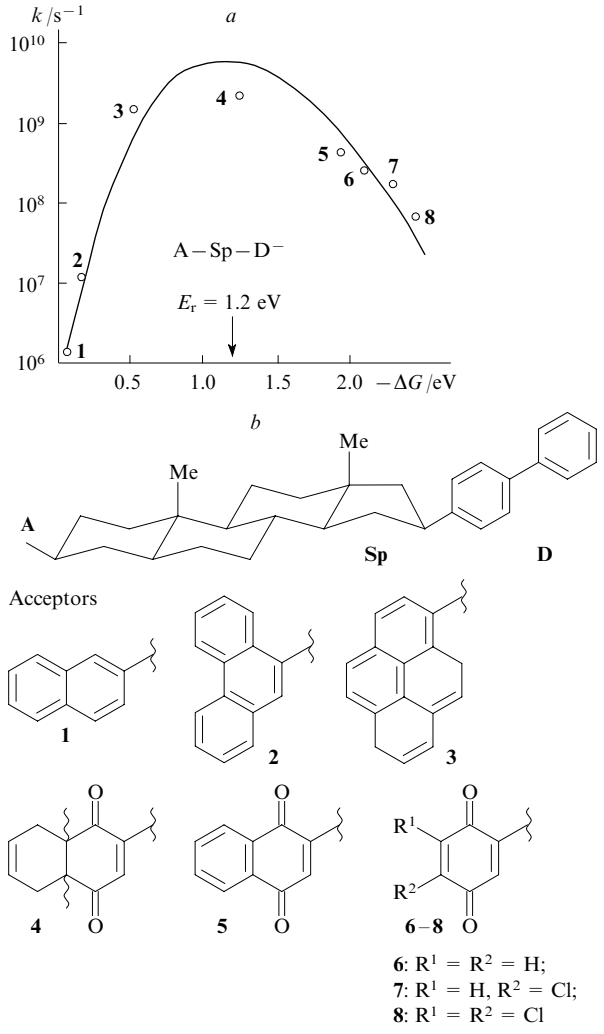


Figure 3. The bell-shaped dependence of the rate of intramolecular ET between a donor (phenylbenzene) and an acceptor of the electron density, which are bound by a bridge, on the exothermicity of the reaction (*a*), and the molecular structure of the bridge (Sp) and the acceptors (*b*).[67]

atic measurements of rates of intramolecular photoinduced ET are shown in Fig. 3.[67] These experimental results are well described by Marcus theory taking into account HF vibration reorganization (solid line).

At present, the Marcus free energy gap law is experimentally proved to be true not only for intramolecular ET in liquid media, but also for intermolecular ET in solids and in rigid systems where reactants are motionless.[71–74] Quite recently the characteristic bell-shaped dependence of the ET rates on the exothermicity was ascertained in the experiment for intermolecular ET betweem aromatic amines (as donors) and coumarins (as acceptors) in micellar solution.[75] The previous measurements for the same series of DA pairs carried out in polar solvents showed Rhem–Weller's plateau. The inverted dependence of the rate on the free energy was also observed for the proton transfer reaction.[76]

Numerous experimental corroborations of the free energy gap low did not cancel objections against its universality. Till now there is no criterion allowing one to predict the existence of either only inverted or only normal region. However at present the Marcus theory can be successfully applied to description of ET processes in different systems. At the same time one should remember that there are other important aspects as well. For instance, mutual diffusion of reactants and possibility of ET at significant distances have to be taken into account upon description of intermolecular ET processes.

Let s consider other commonly discussed mechanisms affecting the ET kinetics and resulting in deviation from the Marcus free energy gap law. For example, it was suggested[62] that excited electronic states of radical ion pairs can play an important role in quenching of fluorescence. Really, in case of strongly exothermic processes the energy of the excited electronic states of ions in the pair can be lower than the energy of the reactants, and the transition into such states can suppress the transition into the ground state of the ion pair. This means that the strongly exothermic reactions, which correspond to the remote part of Rhem–Weller's plateau, are actually not too exothermic. The detailed studies of kinetics of one of the most exothermic reactions, *viz*. of quenching of perylene by tetracyanoethylene in acetonitrile (ACN) solution, showed that the excited states participate in the quenching indeed, and therefore the kinetic rate is much larger than the diffusion one.[77] Below, the processes of quenching of fluorescence due to ET, requiring obligatory account of mutual diffusion, will not be discussed. Experimental and theoretical studies of such processes are considered in detail in several reviews.[6,8]

Another cause of lack of the inverted region can be dependence of the quenching radius on exothermicity of the reaction.[24,26,28,78] Indeed, in the region of low exothermicity, quenching is most efficient when the reorganization energy is small [see Eqn (1)], while in the region of strong exothermicity, the highest rate can be acquired at large reorganization energies. According to Eqn (2), the reorganization energy has to increase with increasing distance between the donor and the acceptor, therefore it can be expected that quenching shifts from the contact pairs to distant ones with increase of reaction exothermicity. In turn, it means that the effective reorganization energy increases with the exothermicity growth and this can result in shift of the inverted region beyond the magnitudes of exothermicity attainable in the experiment.

Missing of the normal region in the processes of charge recombination in DA complexes after excitation in the charge transfer absorption band [29–33, 36, 37, 66, 79, 80] also requires refining their mechanisms. Particularly, one should take into account that the nuclear subsystem is in nonequilibrium state after excitation of the reaction system by a short laser pulse. This can significantly affect kinetics of the following charge recombination, especially if it occurs for a time comparable with the nuclear relaxation time.

IV. Nonequilibrium effects in the ultrafast charge transfer reactions

Development of laser technique remarkably extended experimental capabilities of study of the ET reactions. In the late of 1980s, when a method laser pulse compression to a few tens of femtoseconds was proposed, an opportunity appeared to carry out experiments with femto- and picosecond resolution and to investigate details of elementary acts of chemical transformations in condensed phases. The technique affording such resolution allowed studies of nonstationary spectrally-kinetic phenomena, related to nuclear subsystem relaxation and photoinduced chemical transformations.

The first studies of effects of nonequilibrium of the nuclear subsystem in excited molecules related to the hot luminescence investigations.[81–87] The experimental time dependen luminescence shift evidenced of nonequilibrium of the nuclear subsystem. As expected, the next stage was study of influence of the nonequilibrium on the charge transfer kinetics.[3, 88–95]

In recent years there has been a marked increase in the number of both experimental and theoretical studies of ultrafast ET reactions occurring for tens of femtoseconds[3, 36, 88, 93, 96–110] usually in nonequilibrium regime. Among them are, for example, the experimentally observed ET from aniline molecule to a photoexcited acceptor proceeding in femtosecond area.[111] Another example is the reversible photoinduced transition in ruthenium complexes

$$(NH_3)_5Ru^{2+}(CN)Ru^{3+}(CN)_5^- \rightleftarrows (NH_3)_5Ru^{3+}(CN)Ru^{2+}(CN)_5^-$$

which occurs in aqueous solution in less than 100 fs.[112] The fastest ET processes were observed in synthetic supramolecular systems (the rate constants are from 30 to 10 ps^{-1}) [113] and in the charge recombination reactions in DA complexes after their photoexcitation by a short laser pulse at the frequency of their charge transfer absorption band (rate constants are of 100 ps^{-1}).

Photosynthesizing reaction centres of bacteria and plants represent an additional example of the systems with the ultrafast charge separation at the initial stage. For these systems, the dynamics of the photoinduced electron transfer manifests itself in the absorption and stimulated emission with femtosecond resolution.[114, 115]

Studies of the ultrafast charge recombination revealed a significant role of nonequilibrium of the nuclear subsystem in them.[37, 39–42, 103] Indeed, in case of the ultrafast reaction, relaxation of initial nonequilibrium state of the nuclear subsystem, which has been formed by the exciting pulse, is parallel to the recombination of charges, so the process proceeds in the nonequilibrium regime.

The following features inherent in the ultrafast ET reactions are revealed in systematic investigations:

— there are systems in which ET takes place for times much shorter than the longitudinal relaxation time (τ_L), *i.e.* the time of diffusion solvation [97, 102] (it is known that the longitudinal relaxation time of the solvent determines the bottom limit of the ET time in the theory of thermal ET reactions);[116]

— the ultrafast ET reactions are very sensitive to specificities of the initial nonequilibrium state of the nuclear subsystem including the reactants and the solvent,[117–119] therefore the use of the standard theoretical conceptions (like the transition state theory, the theory of thermal quantum transitions) is not correct for calculation of the major characteristics of the ET process;

— coherent oscillatory effects appearing in periodical modulation of the time dynamics of ET are revealed in investigations of the ultrafast reactions;[95, 102, 120–122]

— dependence of the effective rate constant of ET on the carrier frequency of the exciting pulse (*i.e.* the spectral effect) [93, 94, 106, 109, 123] was experimentally revealed and theoretically explained, it evidences the important role of nonequilibrium of the nuclear subsystem in the ultrafast reactions.

Available experimental data form a basis for development of new theoretical models, capable to describe the major regularities of the ultrafast reactions adequately, as well as for ascertainment of the microscopic mechanisms of these reactions. The first attempts to reveal the contribution of the hot transitions in the ultrafast reactions were made in the studies [39, 42, 124, 125] where the kinetics of reverse ultrafast ET was measured for mixed valence metal complexes. The developed model based on the stochastic point-transition approach allowed quantitative description of the experimental data on quantum yields of the oxidized states of the complexes. The experiments showed that the probability of the reverse ultrafast ET amounts to 0.8 in such complexes, and this fact cannot be explained in the framework of the well known model of Landau–Ziner, for example, although it can be done within the stochastic model.[116] The quantitative agreement between experimental and theoretical results proves the adequacy of the developed conceptions.[42, 124–126] It is worth to note that earlier the stochastic point-transition approach was used for exploration of the hot transitions induced by outer magnetic field in the processes of photoinduced ET [127] and also of the processes of ET from a donor in its singlet state to a paramagnetic acceptor in the polar media.[128]

Failure of traditional approaches for description of the processes of photoinduced ET and the charge recombination in the DA complexes after their photoexcitation at the frequency of the charge transfer absorption band was substantiated in several works.[42, 89, 91, 93, 129] Particularly, it was shown that, in the general case, the stage of optical excitation of the system by ultrashort laser pulse results in formation of the initial nonequilibrium state of the nuclear subsystem that can affect appreciably the kinetics of the further chemical reaction. Description of the process of formation of the nonequilibrium vibrational state on the free energy surface of the excited electronic state has to be a part of the thorough theory of the ultrafast charge transfer.

1. The ultrafast charge recombination reactions in excited donor–acceptor complexes

Systematic studies of the charge recombination reactions in the DA complexes after their excitation by a short pulse at the frequency of the charge transfer absorption

band (see Scheme 2) showed that, firstly, the rate constants of recombination k_{CR} reach values 10^{14} s^{-1}, *i.e.* the processes under consideration proceed over periods of the order of the nuclear relaxation time of the solvent or even faster. Secondly, the rate constants k_{CR} decrease monotonically with increase of the reaction exothermicity [29–33, 36, 37] and do not follow the Marcus free energy gap law. This behaviour of the dependence $k_{CR}(-\Delta G)$ implies that the mechanisms of these reactions differ significantly from the standard mechanism of the thermal ET reactions.

Several approaches were proposed to explain this phenomenon.[40, 57, 88, 104, 130–132] The most efficient approaches are those taking into account the nonequilibrium of the nuclear subsystem of the solvent surrounding the reactant molecules.[40, 57, 88, 130–132] It is assumed within the developed models that, under short pumping pulse, the DA complex transits into its excited state with charge transfer, and this process is accompanied by formation of strong nonequilibrium of the solvent nuclear subsystem. Visually this state can be represented as a wave packet placed on an excited term over the minimum of the term of the ground state (point *B* in Fig. 4). The solvent relaxation corresponds to movement of the packet to the minimum of the term of the excited state (point *C*). In case of weakly exothermic reactions ($-\Delta G < E_{rm}$), in the course of such movement the packet by all means passes the point of the term crossing where the rates of electron transitions increase sharply. Such transitions are called non-thermal or hot. And there may be situations when the recombination of the excited DA complexes is completed at the hot stage, *i.e.* proceeds faster than the relaxation of the solvent.

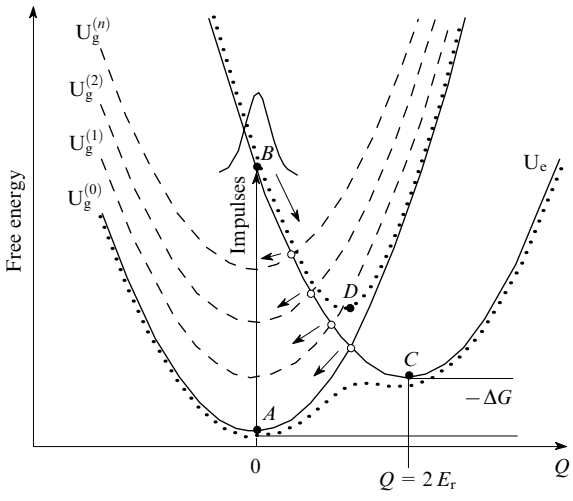


Figure 4. The terms of the excited (U_e) and ground (U_g) states of the DA complex.
The solid lines represent the diabatic terms, the dotted lines show the adiabatic terms, the dashed lines depict vibrational sublevels of the ground electronic state; arrows show the directions of the system relaxation before and after the hot transitions.

Calculation of the effective rate constant within the stochastic model suggested in Ref. 40 taking into consideration the hot transitions reproduce adequately the experimentally observed dependence $k_{CR}(-\Delta G)$. Nevertheless, this model cannot be considered as satisfactory one,[104] because, firstly, well agreement with the experiment can be obtained only for large values of V_{el}, lying far beyond the limits of applicability of the stochastic approach; secondly, the model predicts strongly non-exponential kinetics of decay of the ionic state, while it is close to exponential kinetics in the experiment.[29, 30, 37] The obtained [40] large values for V_{el} ($V_{el} \gg k_B T$) indicate that in the framework of the suggested model the charge recombination in the excited DA complexes has to be considered as a transition between the corresponding adiabatic states induced by the nonadiabatic interaction operator (see Fig. 4). Quasi-classical stochastic point-transition theory of transitions between adiabatic terms induced by the nonadiabatic interaction operator was developed by Shushin.[133] The quantum version of this theory was proposed by Frantsuzov and Tachiya.[104] These authors succeeded in precise reproduction of the experimentally observed dependence of the rate constant on exothermicity of the reaction and in explanation of the absence of the normal Marcus region for the ultrafast reactions in the systems with strong electronic coupling.

However this theory faced significant difficulties. The principal one is that the predicted rates of the charge recombination exceed the medium relaxation rates, and thus, the model has to take into account the nonequilibrium of the solvent nuclear subsystem. Given this nonequilibrium, within the adiabatic model, the authors [88, 130] again received highly nonexponential kinetics of the charge recombination. Besides this model predicts an additional effect, *viz.* decrease in the degree of the charge separation in the relaxation of the solvent. Indeed, after optical excitation, the system is remote from the point of crossing of diabatic terms, and the ionicity of the excited state is close to unity. In the course of relaxation the system state approaches the state corresponding to the minimum of the upper adiabatic term (point *D* in Fig. 4), ionicity of which is close to 0.5. At the same time, an analysis of experimental data showed the the ionicity of the excited states of the DA complexes rather increases with time than decreases.[134]

The mentioned features of the charge recombination kinetics in the DA complexes contradicting the predictions of the models with strong electron coupling have forced to return to non-adiabatic models and to modify them somewhat. One of the modifications is based on taking into account the reorganization of the intramolecular HF vibrations in the DA complexes within the non-stationary perturbation theory,[37, 39] as well as within the stochastic point-transition approach.[57] Participation of the quantum mode in the photoionization/recombination processes results in appearance of vibrational sublevels on the ground and excited terms, which are separated by an energy interval equal to vibrational quantum ($\hbar\Omega$, here $\hbar$ is the Planck constant, Ω is the frequency of the intramolecular vibration). As a result, the process becomes multichannel (see Fig. 4). The starting wave packet in the course of relaxation successively passes through a series of term crossings, undergoing the hot transitions on each of them. The study showed [132] that even for moderate values of the reorganization energy of the intramolecular mode (0.2–0.3 eV) typical of the DA-complexes [33] the probability of the charge recombination at the hot stage approaches unity. Because the transition takes place not on a single crossing, but in quite extended region, the kinetics of the transition approaches exponential form. Simultaneously, the HF mode multiplies the effectiveness of hot transitions, and the agreement with the experiment is achieved at signifi-

cantly lower values of V_{el}, lying within the limits of applicability of the stochastic approach.

Note one more rather important aspect that should be taken into account. As a rule, the vibrationally excited states relax very fast,[135, 136] therefore the theory must necessarily take into consideration the decay of such states. The decay of the final state caused by the intramolecular vibrational relaxation can strongly affect the charge recombination in the DA systems occurring in the solvent-controlled regime (a regime in which the rate of the process depends on the rate of relaxation of the solvent).

An analytical expression is obtained for probability of the hot transition with taking into account the final state decay.[137] For solvents with the same relaxation time the probability of the transition from the ground vibrational state of the reactants to the product excited sate with vibrational quantum number n has a simple form:

$$W_{nt} = \frac{2\pi V_{el}^2}{A_r}\left[1 + 2\pi V_{el}^2\left(\frac{1}{A_r} + \frac{1}{|A_p| f_v}\right)\right]^{-1}. \quad (5)$$

The following designations are used here:

$$A_r = \frac{E_{rm} + \Delta G + n\hbar\Omega}{\tau_L},$$

$$A_p = -\frac{E_{rm} - \Delta G - n\hbar\Omega}{\tau_L},$$

$$f_v = \left(1 + \frac{4B}{\tau_v A_p^2}\right)^{1/2}, \quad (6)$$

$$B = \frac{2E_{rm}k_B T}{\tau_L},$$

τ_v is the vibrational relaxation time. It is easy to see that the vibrational relaxation of the products ($f_v > 1$) accelerates their decay at the hot stage. The measure f_v ranges from 1 to ∞; therefore, it can be demonstrated that the strongest acceleration takes place in the region $|A_p| < A_r$. The values A_r and A_p have meaning of slopes of the reactant and product terms at the point of their crossing. Analysis of the solutions obtained showed that in the solvent-controlled regime the decay of the vibrationally excited state may lead to a significant increase of the probability of the hot transition in a wide range of parameters, except the parameter ranges where this probability is close to unity.[137, 138]

Interpretation of the result obtained is clear enough. It is known that the solvent-controlled ET reactions are controlled by the diffusion transportation of the reactants into the reaction region and by the diffusion removal of species from it. As a result, the populations of the reactants and the products in the vicinity of the term crossing are practically equal. This means that direct and reverse flows are compensated by each other. Therefore the probability of the hot transition may significantly increase upon the final state decay suppressing the reverse reaction flow.[57, 131, 137, 138]

Studies showed that multichannel stochastic model [56, 57, 131, 132, 137, 138] is in full agreement with all the experimental data on ultrafast kinetics of the charge recombination in the DA complexes. This model is based on two-level approximation, which includes the excited electronic state with the charge transfer $|e\rangle$ and the ground state $|g\rangle$ in accordance with Scheme 2 shown above. To account for the reorganization of the HF vibrational modes, a set of vibrationally excited states $U_g^{(n)}$ are considered instead of one state U_g, the excited states in this set differ in energy by the value of the high-frequency vibrational quantum.[139, 140] Thus, one gets a problem with a set of channels of electron transitions (see Fig. 4). In the general case the channels affect each other, *i.e.* the transitions are interrelated. However, this interrelation can be neglected if the condition $\hbar\Omega \gg k_B T$ is met.[141]

Further, we can assume that a short laser pulse with a duration shorter than the solvent relaxation time acts on the complex in the ground state with vibrational subsystem being in equilibrium (in the vicinity of the point A in Fig. 4), resulting in the vertical transfer of a part of the population to the excited term (the vicinity of the point B) and formation of a nonequilibrium wave packet. Further movement of the packet to the minimum of the term U_e reflects reorganization of the classical intrinsic degrees of freedom of the complex and the surrounding solvent induced by the change of the donor and acceptor charges and corresponds to the transition of the system to a new equilibrium position (the vicinity of the point C in Fig. 4). The relaxation of the system is characterized by the autocorrelation function

$$K(t) = \langle \Delta E(t) \Delta E(0) \rangle,$$

where the value

$$\Delta E(t) = U_g - U_e$$

represents the generalized reaction coordinate.[116] The autocorrelation function relates to the solvent relaxation function by simple equation

$$K(t) = 2E_{rm}k_B T X(t).$$

The function $X(t)$ directly relates to the time dependent Stokes shift measurable in the experiment. For an ideal polar solvent, described by the Debye model, the relaxation function has the simple form [116]

$$X(t) = \exp\left(-\frac{t}{\tau_L}\right). \quad (7)$$

Real polar solvents tend to have not one but several relaxation times τ_i.[142–144] These times are usually associated with different relaxation modes, and $X(t)$ is expressed as

$$X(t) = \sum_{i=1}^{m} x_i \exp\left(-\frac{t}{\tau_i}\right), \quad \sum_{i=1}^{m} x_i = 1, \quad (8)$$

where m is the number of the relaxation modes. It is known that the random process with an autocorrelation function of the type (8) can be represented by a multidimensional Gauss random process with the monoexponential autocorrelation function $\exp(-t/\tau_i)$ in each dimension.[145] An independent reaction coordinate Q_i can be associated with each of the dimensions. This can be used to describe the stochastic dynamics of the system by multidimensional equations of the diffusional type.

The diabatic surfaces of the free energy of both the ground and excited states and their vibrational reiterations in the coordinates Q_i ($i = 1, \ldots, m$) can be represented in the form

$$U_g^{(n)} = \sum_{i=1}^{m} \frac{Q_i^2}{4E_{ri}} + \sum_{\alpha=1}^{M} n_\alpha \hbar\Omega_\alpha + \Delta G, \tag{9}$$

$$U_e = \sum_{i=1}^{m} \frac{(Q_i - 2E_{ri})^2}{4E_{ri}}.$$

Here E_{ri} is the reorganization energy of the ith solvent mode, which is related to its statistical weight x_i in the relaxation function (8) by the equation

$$x_i = \frac{E_{ri}}{E_{rm}},$$

$$E_{rm} = \sum E_{ri};$$

Ω_α is the frequency of the intramolecular HF vibrational mode with number α; $n_\alpha = 0, 1, 2, \ldots$ is the number of the vibrational sublevel of the mode α; M is the number the HF modes.

The time evolution of the system can be described by the Liouville stochastic equations [116, 146] for the probability distribution function to find out a species in the vicinity of the point $(Q_1, \ldots, Q_m)$ at the time moment t on the term of the excited state $\rho_e(Q_1, \ldots, Q_m, t)$ and on the set of vibrational sublevels of the term of the ground state $\rho_g^{(n)}(Q_1, \ldots, Q_m, t)$

$$\frac{\partial \rho_e}{\partial t} = \hat{L}_e \rho_e - \sum_n k_n(Q_1, \ldots, Q_m)\left(\rho_e - \rho_g^{(n)}\right), \tag{10}$$

$$\frac{\partial \rho_g^{(n)}}{\partial t} = \hat{L}_g \rho_g^{(n)} - k_n(Q_1, \ldots, Q_m)\left(\rho_g^{(n)} - \rho_e\right) + \tag{11}$$

$$+ \sum_{\alpha=1}^{M} \frac{1}{\tau_v^{(n_\alpha+1)}} \rho_g^{(n'_\alpha)} - \frac{1}{\tau_v^{(n)}} \rho_g^{(n)}.$$

Here $\hat{L}_e$ and $\hat{L}_g$ are the Smoluchowski operators describing diffusion movement on parabolic terms U_e and $U_g^{(n)}$

$$\hat{L}_e = \sum_{i=1}^{m} \frac{1}{\tau_i}\left(1 + (Q_i - 2E_{ri})\frac{\partial}{\partial Q_i} + \langle Q_i^2 \rangle \frac{\partial^2}{\partial Q_i^2}\right), \tag{12}$$

$$\hat{L}_g = \sum_{i,=1}^{m} \frac{1}{\tau_i}\left(1 + Q_i \frac{\partial}{\partial Q_i} + \langle Q_i^2 \rangle \frac{\partial^2}{\partial Q_i^2}\right), \tag{13}$$

$\langle Q_i^2 \rangle = 2E_{ri}k_B T$ is a dispersion of the equilibrium distribution along the i-th coordinate.

The electron transitions between the excited state $|e\rangle$ and the nth vibrational sublevel of the ground state $|g\rangle$ are described by parameters $k_n(Q_1, \ldots, Q_m)$ having the form [116, 146]

$$k_n = \frac{2\pi V_n^2}{\hbar}\,\delta\left(U_e - U_g^{(n)}\right) = \frac{2\pi V_n^2}{\hbar}\,delta\left(z - z_n^{\dagger}\right), \tag{14}$$

$$V_n^2 = V_{el}^2 F_n,$$

$$F_n = \prod_\alpha \frac{S_\alpha^{n_\alpha} \exp(-S_\alpha)}{n_\alpha!}.$$

Here $z = \sum Q_i$ is the collective energetic coordinate of the reaction,

$$z_n^{\dagger} = E_{rm} - \Delta G - \sum_\alpha n_\alpha \hbar\Omega_\alpha$$

are the points of crossing of the terms U_e and $U_g^{(n)}$. The locations of these crossings are determined by a set of the quantum numbers $\{n_\alpha\}$; however, these points can be numbered (using indexes n). This means that $\{n_\alpha\}$ have a single-valued transformation to the set of integers n. The unique correspondence is defined by the inequality $z_n^{\dagger} < z_{n+1}^{\dagger}$. The values F_n are the Franck–Condon factors, $S_\alpha = E_{rv\alpha}/\hbar\Omega_\alpha$ are the Huang–Rhys factors, $E_{rv\alpha}$ is the energy of reorganization of the intramolecular mode α; n'_α ccorresponds to the set of the quantum numbers $n'_\alpha = \{n_1, n_2, \ldots, n_\alpha + 1, \ldots\}$.

First, consider the case where only one mode undergoes the reorganization. In accordance with the model under use (10), (11), it is assumed the single-quantum relaxation mechanism of the HF vibrations operates in the DA complexes, which allows only transitions with an alteration of the quantum number equal to unity $n_1 \to n_1 - 1$, which proceed at the rate $1/\tau_v^{(n_1)}$. It is known that the vibrational relaxation of the polyatomic molecules includes two stages. At the first stage a redistribution of the energy among intramolecular vibrational degrees of freedom takes place. Quantitative information concerning the times of these processes is still limited, it is only known for sure that they can be less than 100 fs.[135] The major cause of the energy redistribution is anharmonicity of vibrations in polyatomic molecules. On assumption that the cubic terms in the anharmonicity are dominant, one can get the following estimation:

$$\tau_v^{(n)} = \frac{\tau_v^{(1)}}{n} \quad (n =, 1, 2, \ldots), \tag{15}$$

i.e. rates of the relaxation transitions $n \to n - 1$ increase fast with the increase of the number of the vibrational sublevel. In the simplest case the pumping pulse can be described by the function

$$E(t) = E_0 \exp\left(i\omega_e t - \frac{t^2}{\tau_e^2}\right), \tag{16}$$

with two parameters, viz. the duration τ_e and the carrier frequency ω_e. Under the assumption that the duration of the pump laser pulse is short the medium can be considered frozen during photoexcitation. In this case the photoexcitation can be considered as a vertical transfer of a part of the equilibrium distribution from the ground to the excited term with good accuracy. Then the initial conditions for the system (10), (11) have the form [94]

$$\rho_e(Q_1, \ldots, Q_m, t = 0) = Z^{-1} \sum_{n_\alpha} \left[\prod_\alpha \frac{S_\alpha^{n_\alpha} \exp(-S_\alpha)}{n_\alpha!}\right] \cdot \tag{17}$$

$$\cdot \exp\left[-\frac{\left(\hbar\delta\omega_e^{(n)} - \sum \widetilde{Q}_i\right)^2 tau_e^2}{2\hbar^2} - \sum \frac{\widetilde{Q}_i^2}{4E_{ri}k_B T}\right],$$

where Z is the normalizing factor,

$$\hbar\delta\omega_e^{(n)} = \hbar\omega_e + \Delta G - E_{rm} - \sum_\alpha n_\alpha \hbar\Omega_\alpha,$$

$$\widetilde{Q}_i = Q_i - 2E_{ri}.$$

The system of the differential equations (10), (11) together with the initial conditions (17) determines the mathematical model for calculation of the kinetics of recombination of the excited DA complexes. Particularly,

the population of the ionic state [$P(t)$] can be calculated as m-dimensional integral of the corresponding distribution function

$$P(t) = \int \rho_e(Q_1, ..., Q_m, t) dQ_1 ... dQ_m . \quad (18)$$

In the studies [57, 131, 132] the system of the differential equations together with the initial condition was solved numerically using the method of the Brownian modelling.[94, 147] Values of some model parameters were determined from the analysis of Raman spectra and the absorption bands of charge transfer. Quite similar model of the charge recombination in the DA complexes was also explored.[56] It is necessary to note that there is an essential difference between the approach developed in the studies [57, 131, 132] and that suggested by Bagchi and Gayathry.[56] The difference is associated with consideration of the local reversibility of the reaction in equations (10) and (11); the approach used in the study [56] excludes it completely. At the same time the local reversibility of the recombination may play significant role especially for the contact ion pairs, to which the excited DA complexes belong, their V_{el} is large enough, and the ET reactions for them proceed in the solvent-controlled regime.

To illustrate efficiency of the multichannel stochastic point-transition model [57, 131, 132, 137, 138] and to ascertain that the considered mechanism operates in the experimentally observed reactions, the developed approach was applied to an analysis of data obtained for the complex Per – TCNE in solution of ACN.[29] The used pulses had duration $\tau_e = 0.57$ ps.[29] The observed signal $\Delta A(t)$ was assumed to be equal to the convolution of the ion pair population and the excitation pulse

$$\Delta A(t) = \left(\pi\tau_e^2\right)^{-1/2} \int_{-\infty}^{t} P(t-\tau) \exp\left(-\frac{\tau^2}{\tau_e^2}\right) d\tau. \quad (19)$$

The results of the modelling are shown in Fig. 5. Note that the found values of the parameters are suitable for many DA complexes.[33] A good quantitative conformity of the results indicate that the considered mechanisms of the ultrafast recombination operate in this system.

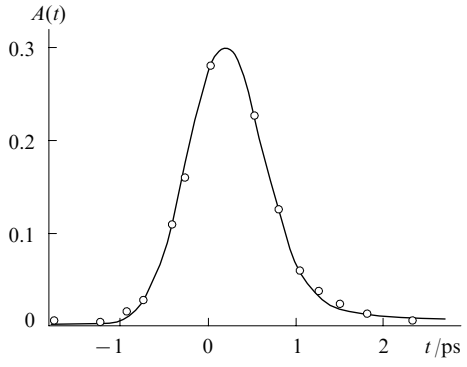


Figure 5. The results of a numerical calculation of kinetics of the signal for the complex Per – TCNE in the ACN solution (the solid line) and the experimental data [130] (dots).
The ACN parameters: three modes with weights $x_1 = 0.5$, $x_2 = 0.4$, $x_3 = 0.1$ and with the corresponding times $\tau_1 = 0.19$, $\tau_2 = 0.5$, $\tau_3 = 5$ ps. The parameters: $T = 300$ K, $\hbar\Omega_1 = 0.1$ eV, $\Delta G = -0.5$ eV, $E_{rm} = 0.7$ eV, $V_{el} = 0.025$ eV, $E_{rv1} = 0.3$ eV, $\tau_v = 0.07$ ps.

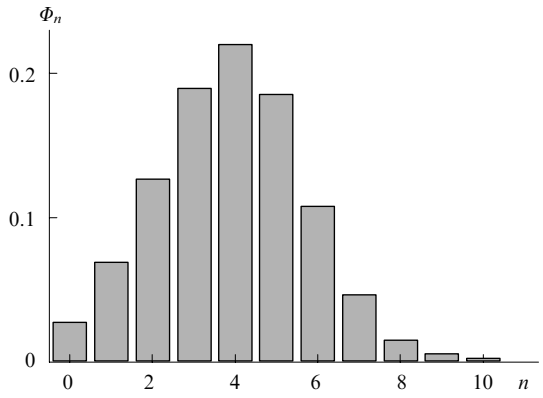


Figure 6. The distribution of products of the hot recombination over the vibrational sublevels $U_g^{(n)}$ of the ground state.
The values for the parameter are given in the caption to Fig. 5.
Φ_n is the probability of formation of the recombination product in a state with n vibrational quanta.

The Huang – Rhys parameter equal to three demonstrates that the recombination in the complex Per – TCNE has essentially multichannel character and involves highly excited vibrational states. This is also illustrated by Fig. 6 where distribution of the recombination products among the vibrational sublevels of the ground state is shown. As can be seen, the most effective transitions are those with generation of 3 – 5 vibrational quanta, $\sim 60\%$ hot transitions correspond to them.

Thus, the multichannel stochastic model, proposed in the studies [57, 131, 132, 137, 138] and taking into account excitation of intermolecular vibrations in the complex and their fast relaxation, is suitable for reproducing the experimental data concerning the ultrafast charge recombination in the DA complexes under certain conditions.

2. Models including reorganization of several intramolecular quantum modes

The most serious examination of the developed multichannel stochastic point-transition model [57, 131] was done for a series of the DA complexes and solvents, for which the following points were studied step-by-step:[132]

— the charge transfer absorption band,

— the kinetics of charge recombination upon excitation by a pulse of the specified carrier frequency,

— the dependence of the charge recombination rate on the excitation pulse carrier frequency,

— effects of polarity and dynamic parameters of the solvents.

This study was based on the experimental data [148] on kinetics of the ultrafast charge recombination reactions in the DA complexes formed by hexamethylbenzene (HMB), pentamethylbenzene (PMB), isodurene (IDU) and trimethoxybenzene as electron donors and TCNE as an electron acceptor in a series of polar solvents [ACN, valeronitrile (VaCN) and octanenitrile (OcCN)], whose diffusion relaxation times differ by more than an order.

The major parameters of the model were explicitly determined in the first two stages on the basis of fitting of the charge transfer absorption band and the kinetics of the charge recombination in a particular solvent upon excitation by a pulse of the given wavelength ($\lambda = 530$ nm). The following parameters were determined from analysis of

Raman spectra and the charge transfer absorption bands: ΔG, E_{rm}, Ω_α and $E_{rv\alpha}$ ($\alpha = 1, \ldots, 10$). The parameters of the electronic coupling V_{el} were found from the time dependence of the ionic state population in the solution of ACN. The two final stages, *viz*. the calculation of the spectral effect and the study of the solvent influence, were carried out without use of adjustable coefficients. Having thus determined the parameters used in the theory, its predictions may be compared with the experimental data on effects of the dynamic characteristics of the solvents and the excitation pulse carrier frequency on the charge recombination.

The studies showed [148] the following:

— the ultrafast kinetics of the charge recombination reactions in the complexes under consideration appreciably deviates the exponential one and can be approximated by a function of the type

$$P(t) = \exp\left[-\left(\frac{t}{\tau}\right)^s\right]$$

the exponent s is in the range from 1.14 to 1.57;

— the effective time of the charge recombination is greatly reduced for all the considered DA complexes with a decrease in the solvent diffusion relaxation time;

— the effective rate constant in slowly relaxing solvents depends on the excitation pulse carrier frequency for several DA complexes, *i.e*. the spectral effect (which represents influence of the pumping pulse frequency on the rate of a photochemical reaction) is observed;

— the solvent effect on the charge recombination reaction is of the same kind for the DA complexes IDU – TCNE, PMB – TCNE and HMB – TCNE, while the spectral effect is manifested in different ways, or not shown at all. In the VaCN solution the spectral effect measured under the influence of pumping pulses at 480 and 620 nm turns negative for the complex IDU – TCNE (*i.e*. increase in the pumping pulse frequency results in decrease of the recombination rate), while for HMB – TCNE it is positive (*i.e*. the recombination rate increases with the increase of the pumping pulse frequency), and for PMB – TCNE it is not observed.

Numerical investigation showed that the model [57, 131, 132, 137, 138] considered above provides a good quantitative agreement with experimental data obtained in the given solvents for the complex IDU – TCNE only (Fig. 7). In case of the complexes PMB – TCNE and HMB – TCNE the model correctly describes a change in the effective rate constants for the ACN and VaCN solutions, but significantly overestimates the rate constant in the OcCN solution. The stochastic model well reproduces non-exponential ultrafast kinetics of the charge recombination reaction, but somewhat overestimates the parameter s.

The conclusion [34] that a single-mode approximation is not sufficient for description of the intramolecular reorganization of the DA complexes is confirmed in the study.[132] The kinetics of the charge recombination in the excited DA complexes is predicted to be significantly faster in the models utilizing the real spectrum of the quantum modes than in the models with a single effective mode. This means that the real spectrum, which includes up to ten active modes, according to the data for several complexes consisting of methyl-substituted benzenes and TCNE,[34, 132] must be used for the quantitative description of the ultrafast reactions. The real spectrum for the charge recombination

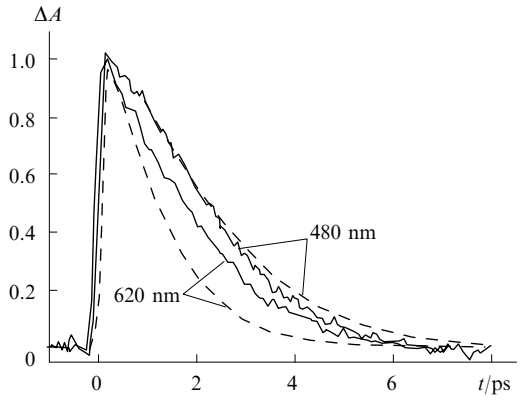


Figure 7. The experimental data (the solid lines) [148] and the results of a numerical modelling (the dashed lines) [132] of the charge recombination kinetics for the complex IDU – TCNE in VaCN.
The wavelength of the excitation pulse is shown near the lines. ΔA is the difference in the absorption with and without the pumping pulse.

reactions is known for few DA complexes, and at present there is no method of its measurement for the photoinduced ET reactions, this causes serious problems in the modelling of these processes.

A way out of this situation was proposed in the study [149] where the following findings were made:

— at a given reorganization energy of the quantum vibrational modes the charge recombination rate increases with the number of the active modes (M);

— this dependence becomes close to saturation near $M = 5$;

— at a fixed M the rate of the charge recombination reaction mainly depends on the total energy of reorganization of the HF modes and weakly depends on their spectrum;

— a universal spectrum including 5 – 10 modes can be used as a good approximation for any DA complex.

The latter conclusion is especially important, because it allows one to model kinetics of ultrafast processes using one of the known spectra as the universal one.

3. The ultrafast reactions of the photoinduced electron transfer. Two reaction coordinates

As shown in a number of studies, the reactions of ultrafast photoinduced ET (see Scheme 3) are characterized by several specific features. One of them is that the locally excited state formed by pumping pulse does not have time to complete the relaxation before the charge separation takes place. This means that the system remembers its initial state (*i.e*. the state before excitation). As a result, the kinetics of the ultrafast photoinduced ET is influenced not only by relative positions of terms of the excited electronic state and the charge transfer state, but also by the positions of the ground state term relative to these two terms. The correct interpretation of such processes is possible only in framework of three-level models (the states $|1\rangle$, $|2\rangle$, $|3\rangle$) and has to include explicit description both of the photoexcitation process and of the subsequent charge transfer.[89, 129]

Another important feature is related to the fact that the charge transfer is a two-stage process. Taking into account that the reorganization of a polar medium is mainly related to the dielectric response to the spatial redistribution of electron density in the DA pair and that the electron density

changes at both stages, one has to introduce two reaction coordinates, corresponding to each of the stages. Within the theory of the linear response of the medium, the reaction coordinate can be represented as a linear combination of coordinates associated with the nuclear degrees of freedom of the medium. In the multidimensional configuration space of the nuclear degrees of freedom of the medium some direction corresponds to each reaction coordinate. An additional characteristic of the kinetics of the ultrafast photoinduced ET is the angle (θ) between the coordinates, corresponding to the stages of the photoexcitation and the electron transfer (Fig. 8).

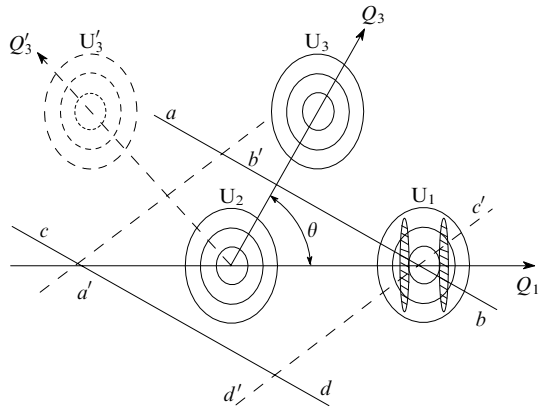


Figure 8. The free energy surfaces.
The solid lines are isolines corresponding to the ground state (U_1), to the locally excited state (U_2) and to the charge transfer state (U_3); the dashed line is the isoline U_3' for the configuration with $\theta > 90^\circ$; the lines of the crossing of the surfaces U_2 and U_3 (U_3'): *ab* (*a′b′*) is for the normal region and *cd* (*c′d′*) is for the inverted region; Q_1 and Q_3 the reaction coordinates corresponding to the optical transition and to ET; the hatched ellipses on the excited state surface are wave packets generated by the excitation pulse with the carrier frequency $\omega_e^{\pm}$.

It was shown [89, 129] that the angle θ significantly affects the kinetics of the ultrafast photoinduced ET, but the question about the physical parameters influencing this angle was not discussed. The answer to this question was given in the studies,[150–154] in which the two- and three-centred models of the spatial redistribution of electron density were developed. These models were used to calculate the angle θ for particular molecular systems. The development of the three-centred (and more-than-three-centred) molecular systems, in which the ET proceeds step-by-step among several centres, was initiated by studies of the processes of the initial charge separation in photosynthesizing centres of bacteria and plants (see, for instance, the studies [155–159]).

At the first approximation, at the photoexcitation stage the spatial redistribution of electron density in the DA pair is attributed to a change in the dipole moment of one of the reactants.

Laser dyes can serve as examples of molecules in which the photoexcitation stage is associated with a significant change in their dipole moment. Those are DCM [4-(dicyanomethylidene)-6-(4-dimethylaminostyryl)-2-methyl-4H-pyrene], Nile red, phenol blue, coumarins C153, C343, C503, C500. In the molecules of DCM, Nile red and phenol blue, the process of the intramolecular charge transfer occurs between amino, dialkylamino and piperidyl groups as the electron donors and nitro, cyano and thiophenyl groups as the electron acceptors, which are connected by a π-conjugated chain.[160] The absorption and fluorescence spectra of these molecules show appreciable solvatochromism, consisting in a bathochromic (red) shift of the spectra (~ 1700 cm^{-1}) with increase of the dielectric constant of solvents. For coumarins C102, C153, C343, and C503 the fluorescence bathochromic shifts are even larger (~ 5000 cm^{-1}) and correspond to the dipole moment changes of 5–10 D for transition from the locally excited electronic state to the ground state.[160–162] If the donor is a large organic molecule (like DCM), the intramolecular charge redistribution in the DA pair can be modelled within the three-centre model.[151, 152] In this case the extended donor is represented by two spheres, while the acceptor is represented by one sphere. The process of the photoinduced ET is considered as a step-by-step transfer of an effective charge among three centres. At the first stage the transfer of the effective charge δ (the part of the transferred charge in the electron charge units) takes place between the first and the second cavities, thus modelling the charge redistribution at the photoexcitation stage resulting in a change of the dipole moment of the donor molecule

$$\Delta\vec{\mu} = \vec{\mu}_e - \vec{\mu}_g.$$

$\Delta\vec{\mu}$ depends linearly on the parameter δ

$$|\Delta\vec{\mu}| = e\delta R_{ab}.$$

At the next stage the effective charge is transferred from the first to the third centre (the transferred charge is $1-\delta$) and from the second to the third centre (the transferred charge is δ) (Fig. 9). The following parameters are principal in this model: R_{ab}, R_{bc} and R_{ac}, the distances by which the charges are transferred, R_a, R_b and R_c, the radii of the spheres modelling the extended donors (the spheres *a* and *b*) and the acceptor (the sphere *c*); α_0, an angle between two directions of transfer of the effective charge; δ, the part of the transferred charge at the photoexcitation stage.

The energies of the reorganization of the medium at each stage (E_{rm1} and E_{rm3}), and the angle between the

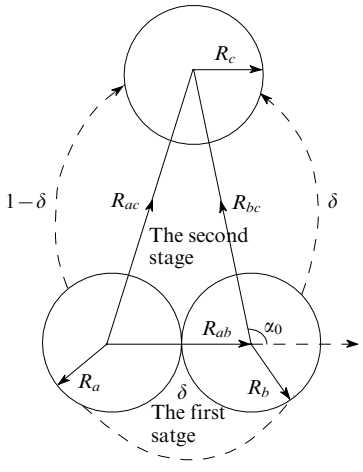


Figure 9. The scheme of the charge redistribution in the process of photoinduced ET in the three-centred system.

reaction coordinates are calculated with account of the chosen geometry within the model of nonoverlapping spheres placed in a continuous dielectric medium,[151, 152]

$$E_{\mathrm{rm1}} = \frac{c_{\mathrm{P}} e^2 \delta^2}{2}\left(\frac{1}{R_a}+\frac{1}{R_b}-\frac{2}{R_{ab}}\right), \tag{20}$$

$$E_{\mathrm{rm3}} = \frac{c_{\mathrm{P}} e^2}{2}\left[\frac{(1-\delta)^2}{R_a}+\frac{1}{R_c}-\frac{2(1-\delta)}{R_{ac}(\alpha_0)}+\frac{\delta^2}{R_b}+\right. \tag{21}$$

$$\left.+\frac{2\delta(1-\delta)}{R_{ab}}-\frac{2\delta}{R_{bc}}\right],$$

$$R_{ac}(\alpha_0) = \sqrt{R_{ab}^2 + R_{bc}^2 + 2\,R_{ab}R_{bc}\cos\alpha_0}\,, \tag{22}$$

$$\cos\theta = \frac{c_{\mathrm{P}} e^2 \delta}{2}\cdot \tag{23}$$

$$\cdot\frac{\left[(1-2\delta)R_{ab}^{-1}+(\delta-1)R_a^{-1}+\delta R_b^{-1}+R_{ac}^{-1}(\alpha_0)-R_{bc}^{-1}\right]}{\sqrt{E_{\mathrm{rm1}}E_{\mathrm{rm3}}}}.$$

A special case with $\delta = 1$ was explored,[150] and it was shown that the angle θ in the model of nonoverlapping spheres is within the range $40^\circ < \theta < 90^\circ$. In the general case the angle θ also depends on δ and α_0. For small δ the angle θ exceeds 90°. The dependences of θ on parameters of the three-centred system are shown in Fig. 10 *a*. It turns out that θ monotonically decreases with the increase of α_0 and δ, with $\theta > 90^\circ$ when $\delta \leqslant \delta_0$. The dependence of δ_0 on the angle α_0 is shown in Fig. 10 *b*.

It must be noted that in the earlier studies [163, 164] also two reaction coordinates were introduced to describe competitive processes of thermal ET from a donor to two different acceptors. Each coordinate was assigned to ET to one of the acceptors of the molecular triad A^1-D-A^2. The principal parameter of the developed theory of the competitive ET processes was the coefficient of correlation between these coordinates. This coefficient coincides with the cosine of the angle θ between two coordinates of the process in the study.[150]

In case of compounds like coumarins and Nile red the dipole moment change at the stage of photoexcitation is not large. Therefore the Lippert – Mataga[165, 166] model may be used to describe intermolecular redistribution of the electron density in such systems. Within this model the donor is considered as a spherical vacuum cavity, in the centre of which a point dipole $\vec{\mu}_{\mathrm{g}}$ is placed. For the two-centred model, the scheme of the spatial charge redistribution is shown in Fig. 11. Within this model the angle θ between the directions of the reaction coordinates corresponding to each stage depends on the orientation of the dipole moment before ($\vec{\mu}_{\mathrm{g}}$) and after ($\vec{\mu}_{\mathrm{e}}$) the optical excitation and on the direction of the subsequent ET specified by the angle α and can be obtained by the formula [153, 154]

$$\cos\theta = \left[f\frac{\mu_{\mathrm{g}}^2-\Delta\mu^2}{R_a^3}-\mathrm{e}\left(\frac{c_{\mathrm{P}}}{3}+f\right)\frac{\mu_{\mathrm{e}}\cos\alpha-\mu_{\mathrm{g}}\cos\gamma}{R_{ac}^2}\right]/ \tag{24}$$

$$/\sqrt{E_{rm1}E_{rm3}}\,,$$

where

$$f = \frac{\varepsilon_0-1}{2\varepsilon_0+1}-\frac{\varepsilon_\infty-1}{2\varepsilon_\infty+1},$$

$\gamma = \arccos(\cos\beta\cos\alpha - \sin\alpha\sin\beta\cos\varphi)$ is the angle between the dipole moment vector for the ground state and the direction of ET (the axis z); φ is the angle between the plane containing the vector $\vec{\mu}_{\mathrm{g}}$ and the direction of ET and the plane including vectors $\vec{\mu}_{\mathrm{g}}$ and $\vec{\mu}_{\mathrm{e}}$ (Fig. 11).

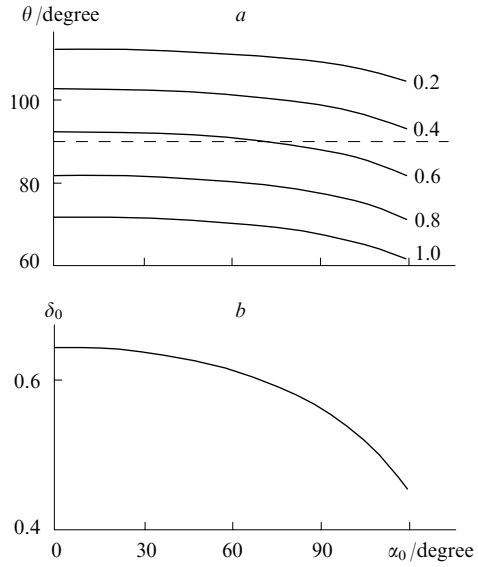


Figure 10. The dependences of the angle θ (*a*) and the parameter δ_0 (*b*) on the angle α_0.
The numbers placed at the curves are the magnitudes of the parameter δ. The parameter δ_0 is a solution of equation (23) for $\theta = 90^\circ$. The calculation parameters are $R_a = R_b = R_c = 3.5$ Å, $R_{ab} = 7$ Å, $R_{bc} = 10$ Å, $\varepsilon_\infty = 1.81$ and $\varepsilon_0 = 37.5$ for ACN.

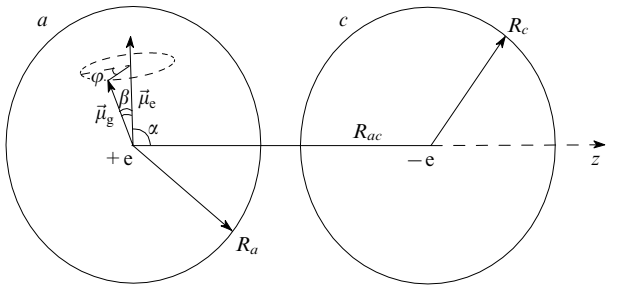


Figure 11. The two-centred scheme of the charge density redistribution in the course of photoinduced ET.
R_a and R_c are the radii of the spherical cavities modelling the donor and the acceptor, respectively; R_{ac} is the distance between the sphere centres; α the angle between the dipole moment of the excited donor and the direction of the charge transfer. The angle φ determines the orientation of the dipole moment $\vec{\mu}_{\mathrm{g}}$ relative to the axis z and $\vec{\mu}_{\mathrm{e}}$.

The energy of the medium reorganization is calculated at each stage within the approximation of two nonoverlapping spheres in the continuous dielectric medium. The reorganization energy at the stage of photoexcitation with inclusion of change in the dipole moment ($\Delta\vec{\mu}$) is calculated using the Onsager model [167] by the following formula:[165, 166, 168]

$$E_{rm1} = f\frac{\Delta\vec{\mu}^{\,2}}{R_a^3}. \qquad (25)$$

An expression for the energy of reorganization $E_{\rm rm3}$ caused by ET at the second stage can be obtained analogously to the expression (25) and has the following form [154]

$$E_{\rm rm3} = \frac{c_{\rm P}e^2}{2}\left(\frac{1}{R_{\rm c}}+\frac{1}{R_a}-\frac{2}{R_{ac}}\right)+\frac{f\mu_{\rm e}^2}{R_a^3}+\left(\frac{1}{3}c_{\rm P}+f\right)\frac{e\mu_{\rm e}\cos\alpha}{R_{ac}^2}. \qquad (26)$$

The dependences $\theta(\alpha)$ for various molecular systems are shown in Fig. 12. As can be seen, the spatial orientation of the dipole moment $\vec{\mu}_{\rm g}$ relative to $\vec{\mu}_{\rm e}$ and z specified by the angle φ significantly affects the angle θ. Particularly, when $\varphi = 180^\circ$ (the dashed lines in Fig. 12) it is significantly smaller than for $\varphi = 0$ (the solid lines). Besides, in case of the parameters typical of coumarins C102 and C343 (curves *4* and *5*), the angle θ does not exceed 90° for any directions of ET, although there are donors (curves *1–3*), for which $\theta > 90^\circ$ in the region $0 < \alpha \leqslant \alpha^*$ [here α^* is the solution of equation (24) when $\theta = 90^\circ$]. When φ increases the critical angle α^* decreases and reaches its lowest value at $\varphi = 180^\circ$. As it was shown, the values of θ and α^* change a little bit on going from ACN to VaCN.

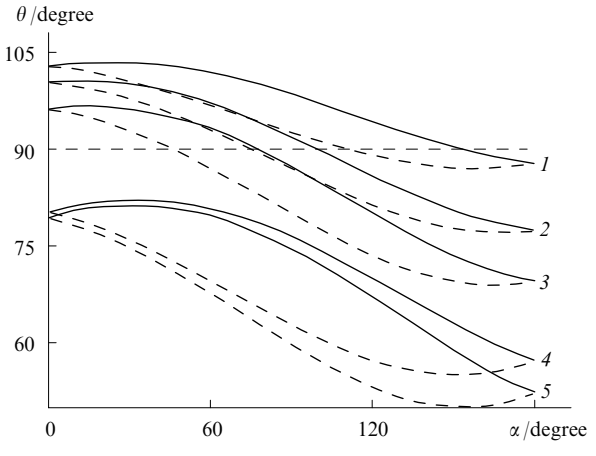


Figure 12. The dependences of the angle θ on the ET direction (α) in the ACN solution.
(*1*) Nile red, (*2*) C153, (*3*) C503, (*4*) C102, (*5*) C343. The solid lines correspond to $\varphi = 0$; the dashed lines correspond to $\varphi = 180^\circ$; other parameters are: $R_c = 3$ Å, $R_{ac} = R_a + R_c + \Delta R$, $\Delta R = 3.62$ Å.

In the simplest case the non-stationary perturbation theory with expansion in terms of matrix elements of the optical (V_0) and nonradiative ($V_{\rm el}$) transition [93] was used to calculate the rates of the photoinduced ET.[150–154] The analytical expression for the rate constant of the photoinduced ET (k_0) is obtained in a form that allows taking into account not only the arbitrary nature of the dielectric constant of the polar environment, but also the influence of both classical and quantum intramolecular vibrations on ET. The spatial charge redistribution takes place at both stages (*viz.* in the phtoexcitation and in subsequent ET) of the process of photoinduced ET; therefore, the kinetics of the whole process explicitly depends on the angle between directions of the coordinates of these processes, as well as on the spectral characteristics of the exciting pulse (*i.e.* on the carrier frequency $\omega_{\rm e}$ and the duration $\tau_{\rm e}$).

The approximate equation for the rate constant of the photoinduced ET in the limit of short laser pulse (k_0), strong coupling with the medium and high temperatures ($k_{\rm B}T \gg \hbar\omega_m$, where ω_m is the characteristic frequency of the classical modes) has a quite simple form

$$k_0(t) = \frac{V_{\rm el}^2}{\hbar P}\frac{\sqrt{2\pi}}{\sigma_{\rm h}(t,\theta)}\sum P_n\,\frac{\exp(-S_3)S_3^m}{m!}\cdot \qquad (27)$$

$$\cdot\exp\left\{-\frac{\left[Q_m^* - Q_n(t,\theta,\omega_{\rm e})\right]^2}{2\sigma_h^2(t,\theta)}\right\},$$

$P = \sum P_n$ is the population of the locally excited electronic state,

$$P_n = \frac{\pi V_0^2\tau_{\rm e}}{\hbar\sigma_0}\,\frac{\exp(-S_1)S_1^n}{n!}\exp\left[-\frac{(\hbar\delta\omega_{en})^2}{2\sigma_0^2}\right]$$

is the probability of the optical transition with absorption of n high-frequency quanta; S_1 is the Huang–Rhys factor for the transition from the first electronic state to the second one; S_3 is the Huang–Rhys factor for the transition from the third electronic state to the second. The quantity

$$Q_m^* = E_{\rm r3} + \Delta G_3 + m\hbar\Omega_3$$

defines the line of crossing of the potential energy surfaces corresponding to the locally excited state and the charge transfer state; the quantity

$$Q_n(t,\theta,\omega_{\rm e}) = 2E_{\rm rm13}(\theta)\left(1+\frac{\hbar\delta\omega_{en}k_{\rm B}T}{\sigma_0^2}\right)X(t) \qquad (28)$$

describes movement of the maximum of the wave packed created by the pumping pulse;

$$\hbar\delta\omega_{en} = \hbar\omega_{\rm e} - E_{\rm r1} + \Delta G_1 - n\hbar\Omega_1\,,$$

$$\sigma_{\rm h}^2(t,\theta) = 2E_{\rm r3}k_{\rm B}T - \left[\frac{2E_{\rm rm13}(\theta)k_{\rm B}TX(t)}{\sigma_0}\right]^2,$$

$$\sigma_0^2 = 2E_{\rm r1}k_{\rm B}T + \hbar^2\tau_{\rm e}^{-2},$$

$$E_{\rm rm13}(\theta) = \sqrt{E_{\rm rm1}E_{\rm rm3}}\cos\theta,$$

$$E_{ri} = E_{{\rm rlf}i} + E_{{\rm rm}i}$$

is the total reorganization energy corresponding to the transition between the locally excited state and the state i; $E_{{\rm rlf}i}$ is the reorganization energy of the low-frequency vibrational mode; $-\Delta G_1$ and $-\Delta G_3$ are the parameters of the exothermicity of the first and second stages.

Some of the time dependences $k_0(t)$ for the two-centred model are shown in Fig. 13. The characteristics of the real molecules of cumarins C503 (variant *1*) and C102 (variant *2*) were used as the parameters in this model, their values were estimated in semi-empirical calculations at the ZINDO/S level. The dipole moments of the ground and locally excited states of coumarins obtained in these calculations agree well with the experimental values.[160]

As seen from Fig. 13, two characteristic regimes can be differentiated in kinetics of the photoindiced ET, those are the non-thermal (k_0 is changed with time) and thermal (steady-state) regimes. The photoexcitation frequency

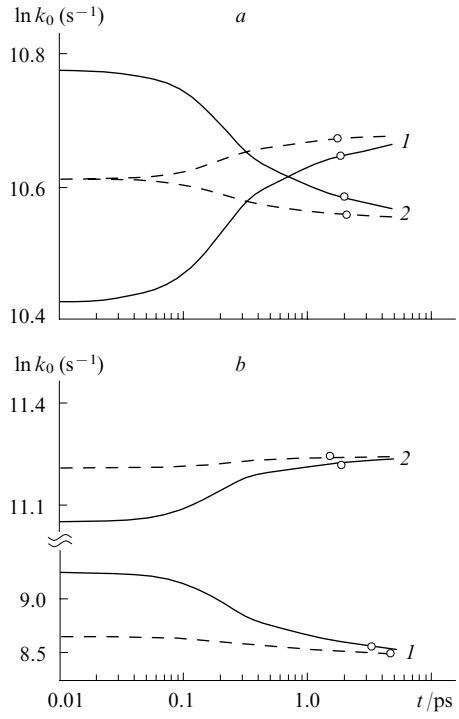


Figure 13. The time dependences of logarithm of the rate constant $k_0(t)$ in ACN.
(*a*): $\alpha = 30^\circ$, $R_{ac} = 12.1$ Å, variant *1*, $\Delta G_3 = -1.2$ (*1*), -2.25 eV (*2*); (*b*): $\alpha = 120^\circ$, $R_{ac} = 11.4$ Å, variant *2*, $\Delta G_3 = -0.75$ (*1*), -2.0 eV (*2*). Other parameters are: $\varphi = 0$, $\tau_e = 50$ fs, $T = 300$ K, $V_{el} = 0.004$ eV, $R_c = 3$ Å. The two-centred model. The times on which the excited state population decreases to 1% are shown by dots.

affects the type of the time dependence of the rate in the non-thermal regime only. The solid and dashed lines in Fig. 13 correspond to the excitations at the frequencies ω_e^+ and ω_e^-, which relate to the excitation at the half-height of the absorption band to the right (ω_e^+) and to the left (ω_e^-) from its maximum. The lines of series *1* describe ET proceeding in the normal Marcus region ($-\Delta G_3 < E_{rm3}$), and those of series *2* show it in the inverted region ($-\Delta G_3 > E_{rm3}$). Configurations of the surfaces U_i ($i = 1, 2, 3$) correspond to $\theta > 90^\circ$ (Fig. 13 *a*) and $\theta < 90^\circ$ (Fig. 13 *b*). Curves *1* describe the case where the 'red' (ω_e^-) and 'blue' (ω_e^+) wave packets arise far from the line of the term crossing (the line a' in Fig. 8), while curves *2* correspond to the case when the wave packets are on opposite sides of the line (the line *b* in Fig. 8). In the first case the rate $[k_0(t)]$ increases, and in the second case it decreases. For $\alpha > \alpha^*$ the kinetics of ET in both variants (*1* and *2*) qualitatively coincides, as shown in Fig. 13 *b*. The rate $[k_0(t)]$ decreases with time in the normal Marcus region and increases in the inverted region. Thus, the geometry of the DA pair and the type of the intramolecular redistribution at the photoexcitation stage may significantly affect the kinetics of photoinduced ET.[152,153] As it is seen, with the change in the angle θ the rate can vary by two orders of magnitude in the normal Marcus region and by an order of magnitude in the inverted region.

As calculations showed, the chemical process may finish before the steady-state (thermal) regime is settled, and therefore a correct description of the non-thermal stage of photoinduced ET is of primary importance. If photoinduced ET proceeds in essentially non-stationary regime, its kinetics may strongly depend on the pumping pulse frequency and on the angle between the directions of the photoexcitation and the subsequent ET.

V. The spectral effect

The capabilities of the modern laser spectroscopy allow studies of the photoinduced reactions of charge transfer and charge separation, which occur over periods of the order of tens of femtoseconds. At present, a series of systems are known, for which their characteristic reaction times are comparable with the vibrational relaxation time. A dependence of the rate of the charge recombination on the excitation pulse frequency is observed for such systems. It is a characteristic feature of the processes of this class, implying the significance of the nonequilibrium of the nuclear subsystem. Therefore the spectral characteristics of the excitation pulse (the carrier frequency and the duration) must be taken into account in the study of the ultrafast ET.

It should be noted that the approach in which the control of the reaction is carried out by varying the spectral characteristics of the excitation femtosecond pulse seems very promising. Different modifications of chirping (of time dependences of the pumping pulse carrier frequency)[15,169,170] and variation of the duration and the carrier frequency of the femtosecond laser pulse[94,171] are used most frequently to this end. The possibility to control the electronic and nuclear movement by variation of the electron coupling between two electronic excited states, one of which is radiative and the other is radiationless, is under discussion in literature.[172] This approach may be fruitful for strong pulses, when there is a strengthening of quantum beats. The period of the beats is determined by the system dynamics exclusively and does not depend on the intensity and the duration of the excitation pulse. Therefore the excitation by a strong pulse can be considered as an attractive instrument to produce molecular systems with strong electron coupling, which can supplement the broadband absorption spectroscopy of the transition process.[173] The major results of the theoretical and experimental studies,[93,94,106,109,148] which concern the influence of characteristics of the excitation pulse, and, particularly, of the pumping pulse carrier frequency, on rates of the ultrafast recombination reaction in the DA complexes and photoinduced charge transfer, are considered below.

The DA complexes in polar solvents are most convenient for such studies. The width of the charge transfer bands for many of such complexes exceeds manifold the spectral width of the excitation pulse, allowing one to vary the excitation pulse carrier frequency in a wide range. The dependence of the ET effective rate constant on the excitation pulse carrier frequency (the spectral effect) was observed by Vauthey and co-workers[94,106,109] in the experiment and explored theoretically.[93,94] Unfortunately, only a few works[94,106,109,148] reporting data on measurements of the spectral effect[94,106,109,148] have been published by the present time. For the first time the spectral effect was observed in the course of charge recombination in the DA complex consisting of 1,2,4-trimethoxybenzene (as a donor) and dianhydride of pyromellite acid (as an acceptor) in the VaCN solution.[106] The measurements showed that increase of the excitation pulse wavelength from 400 nm to 550 nm results in the decrease of the lifetime of the excited state from 1 ps to 680 fs. Because $\Delta G = -1.7$ eV for this reac-

tion, undoubtedly, the charge recombination reaction proceeds into the inverted Marcus region, for which the theory predicts [93] the negative spectral effect (*i.e.* the effective rate decreases with the increase of ω_e), close in magnitude to that found in these experiments. The significant spectral effect was also observed in the recombination reaction in the excited complexes of HMB and IDU with TCNE in polar solvents.[94, 148]

Even earlier, the dependence of the quantum yield of free ions on the excitation pulse wavelength was revealed in the experiment for the DA complexes between alkylbenzenes and TCNE in dichloromethane.[171] For example, the 100-fold increase in the quantum yield of free ions was observed in the DA complexes pentamethylbenzene (PMB)–TCNE upon the change in the excitation wavelength from 530 to 400 nm. This effect was attributed to the excitation of so-called accidental DA pairs, characterized by the charge transfer over long distances (1 nm or more) and by a very weak absorption at the blue edge of the charge transfer band. These experimental data supplemented the study [148] devoted to kinetics of the excited states, and the yield of free ions was very low (about $10^{-6}-10^{-4}$).

Initially, the theory of the spectral effect was developed for the process of the charge recombination in the excited DA complexes, characterized by a single charge transfer absorption band.[88, 93, 94, 109, 150, 174] It was based on the two-level approximation (including the ground state and the charge-transfer state), included the explicit description of the photoexcitation process, used realistic models of the medium and took into account the reorganization of both the classic and quantum intramolecular vibrations in the DA complexes.

The quantitative estimation of the effect of the excitation pulse carrier frequency on the kinetics of the charge transfer can be made from comparison of the effective rates of the process (k_{ef}) upon excitation at two frequencies, for example, at $\omega_e^{\pm}$ (Refs 93 and 94),

$$\phi = \frac{k_{ef}(\omega_e^+) - k_{ef}(\omega_e^-)}{k_{ef}(\omega_e^-)}, \tag{29}$$

where the frequencies

$$\hbar\omega_e^{\pm} = E_r - \Delta G \pm 2(E_r k_B T \ln 2)^{1/2} \tag{30}$$

correspond to the half-height of the absorption band to the right (ω_e^+) and to the left (ω_e^-) from its maximum. The quantity ϕ, reflecting nonequilibrium of the nuclear subsystem, can be a characteristic of the degree of the nonequilibrium. The crucial role of the nonequilibrium stage is also demonstrated by the data shown in Fig. 13. It is seen that the rate constant does not reach the equilibrium value even at 99% conversion.

1. The spectral effect in the charge recombination in the excited donor–acceptor complexes

The study of the dependence of kinetics of the ultrafast charge recombination reaction on the spectral characteristics of the excitation pulse was carried out in the framework of the Fermi golden rule, which was substantiated in the publications.[89, 91] The advantage of this approach consists in that one can obtain an analytical expression for the rate of charge recombination, which takes into account the dynamic of both the photoexcitation and the charge recombination. Besides this approach provides sequential description of reactions in the systems with any dynamic properties of the solvent and any spectrum of the intramolecular vibrations, including high-frequency quantum modes. The main drawback of this approach is that it is strictly applicable only to the cases where the spectral effect is small. However, as investigations of the two-level models of the charge recombination showed that this approach gives qualitatively correct results even in the regions of the parameters that go beyond the limits of its applicability.[94] Therefore the use of this approach is reasonable at the initial stages of investigations of the spectral effect.

The stochastic point-transition approach was used to go beyond the Fermi golden rule,[116] as it has wider area of applicability in terms of electronic transition matrix element.[6] In case of media with several relaxation times, the stochastic point-transition approach results in the problem of multidimensional diffusion on the free energy surfaces with transitions localized in the regions of crossings of the surfaces. Developed numerical methods and algorithms for solving this problem within the two-level model were successfully applied to an analysis of the effect of the pumping pulse carrier frequency on the kinetics of the charge recombination in the excited DA complexes.[94, 174]

In the course of this study it was shown that the spectral effect depends strongly on the dynamic properties of the medium. For instance, it is found within the two-level models that in the polar media characterized by one relaxation time there is only small negative spectral effect (the decrease of the effective rate constant with the increasing excitation pulse carrier frequency), whereas in the media with two relaxation times a large positive spectral effect is predicted for the normal region.[93, 94, 174]

In case of strong electronic coupling between diabatic states, the effect of the excitation pulse carrier frequency on the kinetics of the ultrafast charge recombination reaction in the DA complexes was also studied within the nonstationary Fermi golden rule approach assuming that the transitions between the adiabatic states are induced by the nonadiabatic interaction operator.[88, 130] It was shown that the increase of the excitation pulse carrier frequency always results in the decrease of the effective rate constant irrespective of the dynamic properties of the medium, *i.e.* in this case only the negative spectral effect is predicted.

Thus, with use of different approaches, the quantitative description was obtained for the influence of the spectral characteristics of the excitation pulse on the kinetics of the ultrafast charge recombination reaction in the broad range of parameters, viz. from the extremely weak coupling (using the approaches based on the Fermi golden rule) to the extremely strong coupling (using the adiabatic perturbation theory). A significant region with intermediate magnitudes of the parameters was studied with the use of the stochastic point-transition approach.

The multichannel stochastic model [57, 132] was applied to studies of the spectral effect in the DA complexes formed by the acceptors HMB, PMB or IDU and the donor TCNE in diverse polar solvents. The comparison with the experimental data (see Fig. 7) showed the following:

— the model slightly overestimates the magnitude of the spectral effect in the complexes IDU–TCNE and PMB–TCNE;

— the two-level models are unable to describe the positive spectral effect revealed for the complex HMB–TCNE.

The most probable reason of these discrepancies is that the measured signal is influenced by the wave packet evolution on the terms of the ground and excited states which may result in appreciable difference in kinetics of the excited state population and in the measured signal.

2. The spectral effect in the charge recombination in the excited donor-acceptor complexes with two absorption bands

The spectral effect from variation of the excitation carrier frequency within a single absorption band has been considered above. Upon excitation of the DA complexes into different electronic states corresponding to different absorption bands, the spectral effect acquires essentially new features.

The study of the charge recombination kinetics for a complex consisting of 1,2,4-trimethoxybenzene (TMB) and TCNE was carried out in a series of polar solvents by Vauthey and co-workers.[148] This complex has two charge transfer absorption bands with maxima at wavelengths of 655 and 434 nm, respectively (Fig. 14). The study of the kinetics of the recombination of the photoexcited complex in ACN revealed that it proceeds in two stages, the first one is fast, the second is slow. In more viscous solvents the reaction is completely finished at the fast stage and does not depend on the wavelength of the excitation pulse. The decay of the charge transfer state after excitation at 620 nm has the effective time 30–80 fs in the ACN solution, the signal is attenuated in ~ 0.5 ps practically to zero. Upon excitation of the complex TMB–TCNE by the pulse at 480 nm the two-stage character of the decay kinetics is most prominent: the first stage has the time as short as in the former case, whereas the second stage is slow with the characteristic time much larger than 100 ps.

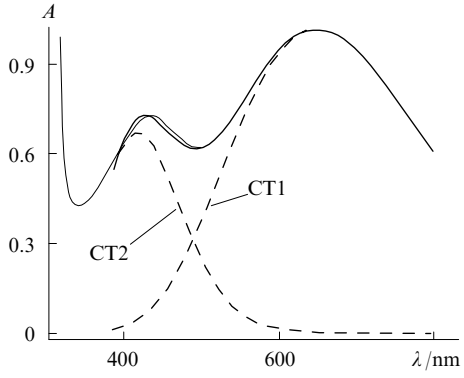


Figure 14. The stationary optical absorption spectrum of TMB–TCNE in ACN (the solid line) and its approximation by a sum of two bands (the thickened line).
The bands CT1 and CT2 are shown by the dashed lines.

It is natural to assume that the second absorption band (Fig. 14) corresponds to the transition to the second excited state of the DA complex. The recombination from the second excited states is possible, but because of its high exothermicity it is less probable than the internal conversion into the first excited state. Thus, it is expected that the charge recombination always proceeds from the first excited state irrespective of the wavelength of the excitation pulse.[148] In accordance with this conclusion, a model for this process in the complexes possessing two charge transfer absorption bands was developed in the study.[175] The model involves three electronic states, *viz*., the ground and the first and second excited states. The chosen model represents an adaptation of the earlier developed model[132] to the complexes with two excited states.

The evolution of the system with time is described within the stochastic point-transition approach generalized to the case of a multilevel system. Most of the energetic parameters of the model are obtained by an approximation of the optical absorption spectrum of the complex under consideration (Fig. 14). The approximation of the optical spectrum of the complex TMB–TCNE was performed analogously to that carried out in the study.[132]

The model reproduces quantitatively the experimental data for the time interval considered (Fig. 15). It is necessary to note that at times >0.5 ps a plateau arises, which was interpreted as the thermal stage of the charge recombination within the model in use. The height of the plateau is determined by the relative number of complexes that avoided the hot recombination. The effective time of thermal stage of the recombination is significantly larger (50 ps) than the time of the hot stage. The experiment also shows that the population of the ionic state is practically invariable in the time interval from 0.5 to 100 ps,[148] *i.e*. the characteristic time of the reaction is much larger than the estimated time of 50 ps. Apparently, this difference is caused by ion solvation neglected by this theory. As a result of the ion solvation proceeding within picoseconds the interionic distance increases, hence, the parameter of the electron coupling between the ground and excited states decreases, and the thermal recombination retards. Figure 15 shows the kinetics of the recombination of the complexes excited by pulses with wavelength of 530 nm. The results of this calculation are also in good correspondence with experimental data.

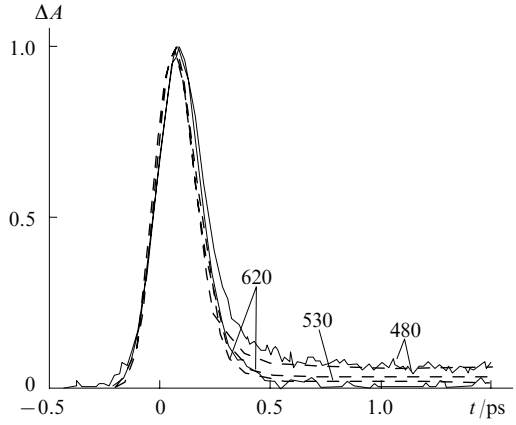


Figure 15. The time dependence of the excited state population of the complex TMB–TCNE in ACN.
The thin solid lines correspond to the experimental data, the dashed lines represent the results of the numerical modelling, the numbers are the wavelengths of the pumping pulses, in nm.

Calculations of the charge recombination kinetics in the complex TMB–TCNE in 'slower' solvents (VaCN and OcCN) showed that the effectiveness of the hot stage increases, and the thermal stage becomes unobservable, which agrees with the experimental data.[148] This is expected because the probability of the non-thermal transition at each term crossing increases with increasing the solvent

relaxation time.[42] This confirms the suggestion that the experimentally observed kinetics of the charge recombination in the excited complexes TMB – TCNE in the solution of ACN[148] is a result of two stages, the hot and thermal ones. Thus, the experimental results attest to non-thermal mechanism of this process in the excited DA complexes.

Evidently, the reason of the fact that the two-stage kinetics of the recombination is observed only in the complexes with two charge transfer absorption bands consists in the following.[175] The donor – acceptor complexes are quite labile systems existing in several quasi-equilibrium configurations. The complexes possessing only one charge transfer band mainly absorb radiation in configurations with the largest electronic matrix element for transition to the ionic state. This seems to be natural assumption, as the probability of absorption is proportional to a square of the matrix element. When the matrix element is large, the charge recombination is ultrafast, and it is already completed at the hot stage. The complexes with two absorption bands have different optimal geometries corresponding to a maximal magnitude of the electronic matrix elements for the transitions to the first and second excited states. As result, the DA complex that was excited to the second excited state and underwent the ultrafast non-radiative transition to the first excited state has non-optimal geometry for the subsequent charge recombination. A smaller magnitude of the transition matrix element causes non-complete charge recombination at the non-thermal stage; therefore, the thermal stage of the recombination becomes observable.

3. The ultrafast processes of charge transfer from the highest excited states. Porphyrins

In accordance with the rules of Vavilov (about independence of the quantum yield of emission on the excitation light wavelength) and Kasha (about emission by molecules from the lowest excited states of a given multiplicity only), the photochemical processes must occur with participation of the lowest electronic excited states only. This is a consequence of the ultrafast internal conversion of higher excited states to the lower ones. Violations of both rules can be expected in case of ultrafast photochemical processes capable to compete with the internal conversion. The only question is what is the scale of these violations.

In the example considered in the previous section these rules are violated only partially, because irrespective of the excitation pulse wavelength, the charge recombination proceeds from the first excited state only, although at different rates. Violations of both rules are observed in the photochemical processes proceeding with participation of higher excited states. All the known processes of this type were observed for porphyrin derivatives. The molecules of these compounds turned out to be most attractive, because their second excited states (S_2) have quite long lifetimes (1 – 3 ps) and large transition dipole moments, that allows one to observe not only fluorescence but also its quenching by diverse electron acceptors.[176 – 180] Moreover, on the basis of such molecules some systems were created capable to operate as molecular switches.[181] For this purpose, the triads were synthesized which included a molecule of zinc porphyrin and two acceptors bound to the opposite sides of the porphyrin ring by covalent bonds. The acceptor parameters were such that the state S_1 was quenched due to the electron transfer to one of the acceptors, and the state S_2 was quenched due to the electron transfer to the other.[181] In such a system, the direction of ET may be controlled by variation of the excitation pulse wavelength populating either the state S_1 or the state S_2.

The ultrafast recombination to the state S_1 took place in all the studied processes of quenching of the state S_2 in the course of intermolecular[180] and intramolecular ET.[181, 182] Most probably, the recombination is hot, because the following sequence of processes was observed:[81]

$$S_2 \rightarrow CS \rightarrow S_1 \rightarrow CS \rightarrow S_0 .$$

Here, the transition $CS \rightarrow S_1$ may proceed in the hot regime only, as it is observed when the energy of the state S_1 is greater than the energy of the state CS.[181] The hot transitions $CS \rightarrow S_1$ are so effective that only 10% – 20% of the formed ionic states are thermalized. The hot recombination reduces selectivity of the processes proceeding from the states S_2 and S_1; therefore, its suppression is desirable for optimization of the operation of the switches. To solve this problem, detailed studies of the hot recombination are required.

The results of experimental and theoretical studies of the charge recombination from the second excited state and the subsequent recombination to the first excited state for a series of supramolecular systems[177 – 179, 182 – 184] will be described in this section. The series consists of derivatives of zinc porphyrins bound by covalent bonds with electron-withdrawing imide groups. The following most important regularities of the charge separation and recombination were revealed in these studies.

Firstly, the rate of attenuation of the fluorescence from the state S_2 is only slightly greater than the rate of rise of the fluorescence from the state S_1.[182] This strongly implies that the decay of the state S_2 is accompanied by population of the state S_1 already at the relaxation stage of a medium and intramolecular vibrations.[182] The hot charge recombination is sharply evident in the supramolecular systems with positive free energy of recombination to the first excited state (the state S_1 lies higher than the charge separated state). Ultrafast growth of the population of the state S_1 is accompanied by its slower decrease in such molecules. The growth is a result of the hot transitions, while the subsequent stage is the thermal decay.

Secondly, the internal conversion $S_2 \rightarrow S_1$ is quite slow in comparison with the charge recombination, so only a few percent of molecules undergo the internal conversion.[182] Taking this into account, one can neglect the internal conversion $S_2 \rightarrow S_1$ in the first approximation.

The experimental data were quantitatively described in terms of the developed model of non-thermal transitions.[184] The model includes the following physical processes. The excitation of the system to the state S_2 is represented as appearance of a wave packet in the vicinity of the minimum of the surface S_2 (Fig. 16). Then the transitions start in the points of the term crossings

$$U_{S_2} = U_{CS}^{(n)},$$

resulting in population of a set of vibrational repetitions of the charge separated states (denoted by the dashed lines in Fig. 16). The formed nonequilibrium state is subjected to several relaxation processes. Firstly, there is intramolecular vibrational relaxation, which leads to the vertical transitions between the neighbouring states (not shown in Fig. 16).

$$U_{CS}^{(n)} \rightarrow U_{CS}^{(n-1)}.$$

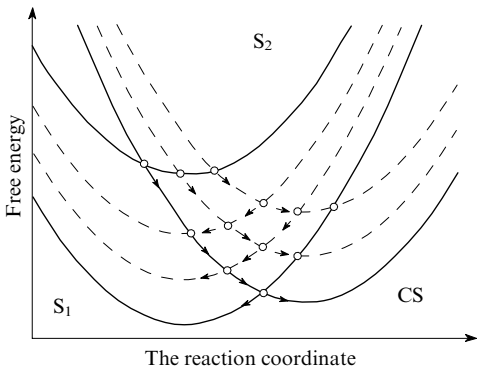


Figure 16. The schematic representation of the free energy curves for the charge separation from the second excited state accompanied by the recombination to the first excited state.
The vibrational repetitions of the respective electronic states are shown by the dashed lines; the arrows show the directions of the medium relaxation and the hot transitions.

Secondly, there is medium relaxation, which is modelled by movement of the wave packet to the minimum of the terms $U_{CS}^{(n)}$. During the relaxation the wave packets move through the term crossing points defined by the equation

$$U_{S_1}^{(m)} = U_{CS}^{(n)},$$

where the hot transitions to the first excited state S_1 take place. It is necessary to note that the intramolecular relaxation in the state S_1, which is modelled by the transitions

$$U_{S_1}^{(m)} \to U_{S_1}^{(m-1)},$$

also plays an important role, because it can increase effectiveness of the hot recombination.[137] Of course, the equilibrium populations of the states S_1 and CS are determined by difference between their energies. However, if the state CS is located below the state S_1, the hot recombination can result in population of the state S_1, significantly greater than its equilibrium magnitude. In this case, the population of the state S_1 increases at short times and decreases at long times.

The time evolution of the system is described by a system of equations for probability distribution functions for the second excited state $\rho_{S_2}(\mathbf{Q}, t)$ ($\mathbf{Q}$ is the vector with the components $Q_1, Q_2, \ldots, Q_N$), for the m-th sublevel of the first excited state $[\rho_{S_1}^{(m)}(\mathbf{Q}, t)]$ and for the nth sublevel of the charge separation state $[\rho_{CS}^{(n)}(\mathbf{Q}, t)]$

$$\frac{\partial \rho_{S_2}}{\partial t} = \hat{L}_S \rho_{S_2} - \sum_n k_n^{CS} \rho_{S_2}, \tag{31}$$

$$\frac{\partial \rho_{CS}^{(n)}}{\partial t} = \hat{L}_{CS}\, \rho_{CS}^{(n)} + k_n^{CS} \rho_{S_2} - \sum_m k_{nm}^{CR} \left(\rho_{CS}^{(n)} - \rho_{S_1}^{(m)}\right) + \tag{32}$$
$$+ \frac{1}{\tau_v^{(n+1)}} \rho_{CS}^{(n+1)} - \frac{1}{\tau_v^{(n)}} \rho_{CS}^{(n)},$$

$$\frac{\partial \rho_{S_1}^{(m)}}{\partial t} = \hat{L}_S \rho_{S_1}^{(m)} - \sum_n k_{nm}^{CR} \left(\rho_{S_1}^{(m)} - \rho_{CS}^{(n)}\right) + \tag{33}$$
$$+ \frac{1}{\tau_v^{(m+1)}} \rho_{S_1}^{(m+1)} - \frac{1}{\tau_v^{(m)}} \rho_{S_1}^{(m)},$$

where $\hat{L}_{CS}$ and $\hat{L}_S$ are the Smoluchowski operators describing diffusion on terms U_{CS}, U_{S_2} and U_{S_1}, respectively. The parameters $k_n^{CS} = k_n^{CS}(\mathbf{Q})$ and $k_{nm}^{CR} = k_{nm}^{CR}(\mathbf{Q})$ characterizing the rates of the transitions between the states U_{S_2} and $U_{CS}^{(n)}$, and also between $U_{CS}^{(n)}$ and $U_{S_1}^{(m)}$ are defined by the expressions

$$k_n^{CS} = \frac{2\pi V_n^2}{\hbar}\, \delta\left(U_{S_2} - U_{CS}^{(n)}\right),$$

$$V_n^2 = V_{CS}^2 F_n,$$

$$F_n = \frac{\left(S^{(CS)}\right)^n e^{-S^{(CS)}}}{n!},$$

$$S^{(CS)} = \frac{E_{rv}^{(CS)}}{\hbar\Omega}.$$

For the transitions between the states CS and S_1 they have more general form

$$k_{nm}^{CR} = \frac{2\pi V_{nm}^2}{\hbar}\, \delta\left(U_{CS}^{(n)} - U_{S_1}^{(m)}\right),$$

$$V_{nm}^2 = V_{CR}^2 F_{nm},$$

$$F_{nm} = \exp\left(-S^{(CR)}\right) n!m! \left[\sum_{r=0}^{\min(n,m)} \frac{(-1)^{n-r}\left(\sqrt{S^{(CR)}}\right)^{n+m-2r}}{r!(n-r)!(m-r)!}\right]^2,$$

$$S^{(CR)} = \frac{E_{rv}^{(CR)}}{\hbar\Omega},$$

where F_{nm}, $S^{(CR)}$ and E_{rv} are the Franck–Condon factors, the Huang–Rhys factors and the energy of reorganization of the effective high-frequency vibrational mode, respectively

The single-quantum mechanism of the HF mode relaxation is adopted here; the transitions $n \to n-1$ have the rates $1/\tau_v^{(n)}$. Naturally, the ground vibrational state is stable. The dependence of the relaxation time on the number of the vibrational state n has a form $\tau_v^{(n)} = \tau_v^1/n$ (Ref. 131).

Then it is assumed that the system in the ground state transits to the second excited state ($S_0 \to S_2$) under action of the short laser pulse. As this excitation is not accompanied by appreciable charge redistribution, the equilibrium state of the polar medium just after excitation is a good approximation. Because the wavelength used in the experiments [182] is close to the red edge of the absorption band $S_0 \to S_2$, it is reasonable to think that the HF mode is in the ground state after the transition. This gives the following initial conditions:

$$\rho_{S_2}(\mathbf{Q}, t=0) = \prod_i \frac{1}{\sqrt{2\pi\langle Q_i^2\rangle}} \exp\left(-\frac{Q_i^2}{2\langle Q_i^2\rangle}\right), \tag{34}$$

$$\rho_{CS}^{(n)}(\mathbf{Q}, t=0) = 0, \tag{35}$$

$$\rho_{S_1}^{(m)}(\mathrm{Q}, t=0) = 0.$$

The equation systems (31), (32) with the initial conditions (34), (35) were solved numerically.

The calculations of the kinetics of CS and CR were carried out for the solution of tetrahydrofuran (THF) at room temperature. The following values of the dynamic parameters of THF [185] were used: $x_1 = 0.443$, $x_2 = 0.557$,

$\tau_1 = 0.226$ ps, $\tau_2 = 1.520$ ps. The relaxation time of the HF mode was assumed to be equal [135, 136] to $\tau_v = 0.030$ ps. The parameters $E_{rm} = 0.5$ eV, $E_{rv} = 0.4$ eV, $\hbar\Omega = 0.17$ eV obtained in the study [179] were also used. The values for the free energies and the electronic matrix elements obtained in the fitting are presented in the study.[132]

The finite time of the instrumental response $\tau_0 = 110$ fs [179] was taken into account to compare the experimental and theoretical dependences. It is assumed that the measured intensity of fluorescence $\Delta A(t)$ is the convolution of the corresponding state population and the function of an instrumental response (19). The signals calculated in this way are shown in Fig. 17.

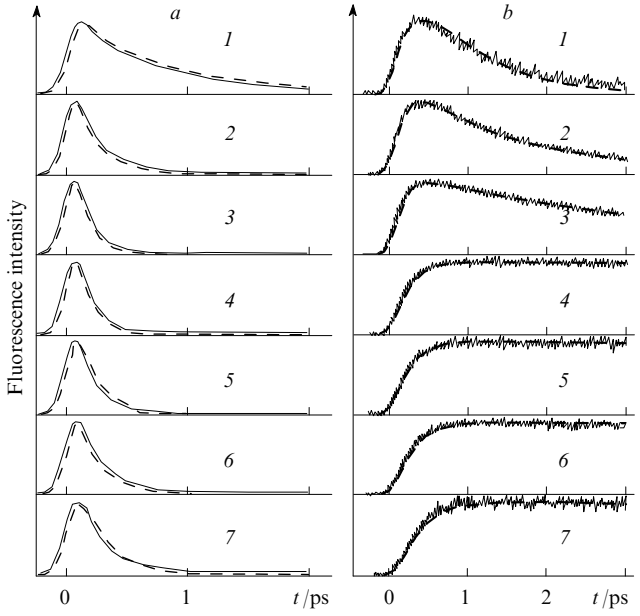


Figure 17. Kinetics of the populations of the states S_2 (*a*) and S_1 (*b*). The solid lines correspond to the experimental data,[182] the dashed lines represent the calculated data.[184] The parameters are: $E_{rm} = 0.5$ eV, $E_{rv} = 0.4$ eV, $\hbar\Omega = 0.17$ eV, $\tau_v = 0.03$ ps, $\tau_e = 0.110$ ps. The complexes of zinc porphyrin with naphthalenetetracarboximide (*1*), pyromellitimide (*2*), 4,5-dichlorophthalimide (*3*), tetrachlorophthalimide (*4*) chlorophthalimide (*5*), phthalimide (*6*), metallaphthalimide (*7*).

Kinetics of the populations of both the excited states S_2 and S_1 was quantitatively reproduced within the same model, which is a substantial argument for adequacy of the suggested model. This is necessary to emphasize that its distinctive feature is the effective hot recombination to the first excited state. This means that the charge separation and the subsequent recombination and vibrational relaxation proceed simultaneously. Although kinetics of the population of the state S_1 is predetermined by the decay time of the state S_2, nevertheless it also depends on the relaxation times of the medium and the intramolecular vibrations. Therefore, the description of the kinetics of the recombination in the first excited state requires solution of the complete dynamic problem, including a great number of vibrational sublevels for three electronic states participating in the process.

In conclusion, recall the ways of suppression of the hot recombination to the state S_1. Those are reduction of the quantity V_{CR}, lowering of the reorganization energy for the vibrational HF mode and decrease of its relaxation rate, increase of the medium relaxation rate.

4. The spectral effect in the reactions of photoinduced electron transfer

Only an effect of the excitation pulse carrier frequency on the kinetics of the charge recombination in the excited DA complexes was studied experimentally. The spectral effect was not observed in the reactions of photoinduced ET. Nevertheless, the results of the theoretical calculations [150–154] evidence that this class of ultrafast ET processes can be a suitable object for experimental studies of the spectral effect. Its magnitude is predicted to be large; therefore, it can be reliably detected in experiment. The strong dependence of the spectral effect on the geometry of the DA pair and the electron density redistribution in it at the stages of photoexcitation and charge transfer can give the lacking information concerning the structure of such pairs.

To illustrate this dependence, the isolines of the spectral effect $\phi(\Delta G_3, \alpha)$ are shown in Fig. 18. The quantity ϕ is calculated within a two-centred model with two different sets of parameters characterizing the geometry and the charge redistribution in the DA pairs, which include laser dyes (coumarin C503, see Fig. 18 *a*; coumarin C102, see Fig. 18 *b*) as the donor. This molecules are characterized by relatively large changes in the dipole moment upon photoexcitation. Their parameters calculated with the semiempirical method ZINDO/S for the ground state geometry obtained in the ZINDO/1 calculations are given in the works.[153, 154] In the two-centred model the geometrical parameters of the intramolecular charge redistribution (the angles φ, β and α) determine the angle θ between the directions of the reaction coordinates, corresponding to the photoexcitation and to the subsequent charge transfer. For instance, the angle θ is always lower than 90° for the pairs with C102 as the donor. In this case, if the exothermicity of the reaction of photoinduced ET is high ($-\Delta G_3 > 1.5$ eV), the spectral effect may be positive only, whereas it is only negative if the exothermicity is low ($-\Delta G_3 < 1.5$ eV). The value $|\phi|$ increases with increasing of

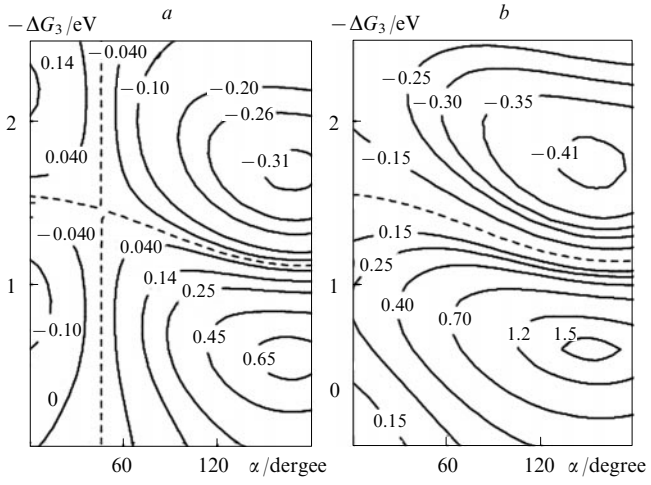


Figure 18. The isolines of the spectral effect $\phi(\Delta G_3, \alpha)$ for the spatial geometry of C503 (*a*) and C102 (*b*) in VaCN.
$\varphi = 0$ (*a*) and 180° (*b*); the dashed line is the isoline of the zero spectral effect. The other parameters are: $\tau_e = 50$ fs, $T = 300$ K, $V_{el} = 0.004$ eV, $R_c = 3$ Å, $R_{ac} = R_a + R_c + \Delta R$, $\Delta R = 3.62$ Å.

the angle α between the direction of charge transfer and the vector $\vec{\mu}_e$. The largest spectral effect is expected for the angles $\alpha > 150^\circ$: ϕ can amount to 1.5 and -0.4 in case of low and high exothermicity of the reaction, respectively.

If the angle between the reaction coordinates corresponding to the excitation and to the charge transfer exceeds 90°, which is characteristic of the DA pairs including C503, the angle α determines not only the magnitude of the spectral effect, but also its sign. In the region where $\alpha < 30^\circ$ (the charge transfer is along the direction defined by the vector $\vec{\mu}_e$) the effect is expected to be positive for the strongly exothermic reactions and negative for weakly exothermic ones.[154]

Therefore, the spectral effect is extremely sensitive to the geometry of the DA system, *i.e.* it depends on the angles α and φ, determining the direction of the charge transfer and the change in orientation of the dipole moment of the donor upon excitation. Thus, this gives an opportunity to obtain the information on the structure of the DA pairs and the pattern of the electron density redistribution in it at the stages of the photoexcitation and the charge transfer from the study of the magnitude and the sign of the spectral effect.

VI. Conclusion

The effect of variation of the excitation pulse carrier frequency within one absorption band on the kinetics of the photoinduced chemical transformations is not large, but it is reliably detected in experiments. The study of this effect opens new opportunities in exploration of detailed microscopic mechanisms for the ultrafast photochemical processes. It is because modern models of chemical reactions include quite many parameters, and the rate constant of a single elementary act can be reproduced within various models, which are often essentially different, and with use of different sets of parameters. This does not allow one to choose the most adequate model. Theories describing the ultrafast processes are subjected to a stricter verification, as such theory has to reproduce non-exponential kinetics characterized by only few parameters. The further refinement of the model can be performed on the basis of comparison of theoretical predictions with experimental data on kinetics of the photoinduced processes in solvents with different viscosity and with various relaxation times. Another trial of the theory can consist in check of its capability to produce a correct description of the dependence of kinetics of a chemical transformation on the excitation pulse frequency. Obviously, the model able to reproduce all of these dependences reflects the microscopic mechanism of the reaction most completly.

At the same time, as the currently available data show, the control of the rate of a photochemical transformation by changing the excitation pulse frequency within one absorption band is not effective. A better approach consists in control of the rate of a photochemical reaction by changing the excitation pulse frequency in such a way that transitions into different electronic states would be excited. As shown by studies of derivatives of porphyrin, in this case the selectivity of the charge separation reaction can approach 100%.[181]

One of the most characteristic features of the charge separation from the second excited state is the hot recombination to the first excited state blocking thermalization of the charge separated state. It is necessary to emphasize that this phenomenon was observed in all performed studies, although there are no many such examples. Besides, effectiveness of the hot recombination in this systems is confirmed by theoretical calculations[184] indicating the universality of this phenomenon. A question emerges in this connection: why does not the hot recombination to the ground state play a determinative role in the processes of charge separation from the first excited state? The reason is that the energy gap between the states S_1 and S_0 is much larger than between the states S_2 and S_1. As result, the recombination to the ground state proceeds, as a rule, in the inverted region, when the recombination rate reaches its maximum after the solvent relaxation and the reaction proceeds mainly in thermal regime. There are only several exceptions to this rule, for example, the DA pair consisting of Per and TCNE represents such exception. The recombination in this pair proceeds in normal region, and, therefore, as studies show, up to 90% of the formed geminate ion pairs recombine at the hot stage.[147, 186] For the reaction of the charge separation from the state S_2, the recombination to the state S_1 is always in the normal region, and the hot transitions have to play the crucial role invariably.

It is necessary to note that an effective hot recombination is observed in transition metal complexes if it proceeds in the normal region. A striking example is represented by pyridine complexes of the type Ru(II)–L–L–Co(III), more than half of them can recombine at the hot stage.[187]

Thus, the experimental and theoretical studies indicate an essential and, sometimes, determinative role of the hot transitions in kinetics of the ultrafast photochemical reactions. As a rule, the hot transitions are undesirable processes decreasing yields of reaction products. In this connection, the problem of their suppression is important. The lately performed studies of the mechanisms of these processes allow one to formulate approaches to solving this problem. The standard methods of control of rates of thermal reactions are inadmissible for the control of efficiency of the hot recombination, because they can lead to opposite results. For instance, on going to viscous solvents, the thermal reactions become slower and simultaneously the effectiveness of the hot transitions increases.

This work was carried out with the financial support of the Ministry of Education and Science (the state contract P1145) and of the Russian Foundation for Basic Research (Project Nos 08-03-00534 and 10-03-97007 r_Volga Region_a).

References

1. A M Kuznetsov *Charge Transfer in Physics, Chemistry and Biology* (Amsterdam: Gordon and Breach, 1995)
2. M V Bazilevskii, V I Faustov *Usp. Khim.* **61** 1185 (1992) [*Russ. Chem. Rev.* **61** 651 (1992)]
3. W Domcke, G Stock *Adv. Chem. Phys.* **100** 1 (1997)
4. *Electron Transfer: from Isolated Molecules to Biomolecules (Advances in Chemical Physics)* Vols 106–107 (Eds J Jortner, M Bixon) (New York: Interscience, 1999)
5. A I Burshtein *Adv. Chem. Phys.* **114** 419 (2000)
6. A V Barzykin, P A Frantsuzov, K Seki, M Tachiya *Adv. Chem. Phys.* **123** 511 (2002)
7. A I Burshtein *Adv. Chem. Phys.* **129** 105 (2004)
8. E Vauthey *J. Photochem. Photobiol. A* **179** 1 (2006)
9. S V Lymar, V N Parmon, K I Zamaraev *Top. Curr. Chem.* **159** 1 (1991)

10. D M Adams, L Brus, C E D Chidsey, S Creager, C Creutz, C R Kagan, P V Kamat, M Lieberman, S Lindsay, R A Marcus, R M Metzger, M E Michel-Beyerle, J R Miller, M D Newton, D R Rolison, O Sankey, K S Schanze, J Yardley, X Zhu *J. Phys. Chem. B* **107** 6668 (2003)
11. Y Shirota, H Kageyama *Chem. Rev.* **107** 953 (2007)
12. P A Troshin, R N Lyubovskaya, V F Razumov *Ros. Nanotekhnol.* **3** 56 (2008) [a]
13. A L Buchachenko *Usp. Khim.* **68** 99 (1999) [*Russ. Chem. Rev.* **68** 85 (1999)]
14. A H Zewail *J. Phys. Chem. A* **104** 5660 (2000)
15. O M Sarkisov, S Ya Umanskii *Usp. Khim.* **70** 515 (2001) [*Russ. Chem. Rev.* **70** 449 (2001)]
16. I R Gould, S Farid *Acc. Chem. Res.* **29** 522 (1996)
17. M Dossot, X Allonas, P Jacques *Chem. – Eur. J.* **11** 1763 (2005)
18. I R Gould, S Farid *J. Phys. Chem. B* **111** 6782 (2007)
19. M G Kuzmin, I V Soboleva, E V Dolotova *J. Phys. Chem. A* **111** 206 (2007)
20. I R Gould, R H Young, L J Mueller, S Farid *J. Am. Chem. Soc.* **116** 8176 (1994)
21. M G Kuzmin *J. Photochem. Photobiol. A* **102** 51 (1996)
22. G J Kavarnos, N J Turro *Chem. Rev.* **86** 401 (1986)
23. K S Peters, J Lee *J. Phys. Chem.* **96** 8941 (1992)
24. T Kakitani, A Yoshimori, N Mataga *J. Phys. Chem.* **96** 5385 (1992)
25. A Weller *Pure Appl. Chem.* **16** 115 (1968)
26. A I Burshtein *Chem. Phys.* **247** 275 (1999)
27. C Zhong, J Zhou, C L Braun *J. Phys. Chem. A* **108** 6842 (2004)
28. M Tachiya, S Murata *J. Phys. Chem.* **96** 8441 (1992)
29. T Asahi, N Mataga *J. Phys. Chem.* **93** 6575 (1989)
30. T Asahi, N Mataga *J. Phys. Chem.* **95** 1956 (1991)
31. H Segawa, C Takehara, K Honda, T Shimidzu, T Asahi, N Mataga *J. Phys. Chem.* **96** 503 (1992)
32. C A Benniston, A Harriman, D Philp, J F Stoddart *J. Am. Chem. Soc.* **115** 5298 (1993)
33. I R Gould, D Noukakis, L Gomez-Jahn, J L Goodman, S Farid *J. Am. Chem. Soc.* **115** 4405 (1993)
34. K Wynne, C Galli, R M Hochstrasser *J. Chem. Phys.* **100** 4797 (1994)
35. K Wynne, G D Reid, R M Hochstrasser *J. Chem. Phys.* **105** 2287 (1996)
36. S M Hubig, T M Bockman, J K Kochi *J. Am. Chem. Soc.* **118** 3842 (1996)
37. O Nicolet, E Vauthey *J. Phys. Chem. A* **106** 5553 (2002)
38. R S Mulliken, W B Person *Molecular Complexes* (New York, London: Wiley-Interscience, 1969)
39. G C Walker, E Akesson, A E Johnson, N E Levinger, P F Barbara *J. Phys. Chem.* **96** 3728 (1992)
40. M Tachiya, S Murata *J. Am. Chem. Soc.* **116** 2434 (1994)
41. W Jarzeba, S Pommoret, J-C Miallocq *Chem. Phys. Lett.* **333** 419 (2001)
42. A I Ivanov, V V Potovoi *Chem. Phys.* **247** 245 (1999)
43. H-J Werner, H Staerk, A Weller *J. Chem. Phys.* **68** 2419 (1978)
44. D V Dodin, A I Ivanov, A I Burshtein *J. Phys. Chem. A* **112** 889 (2008)
45. W F Libby *J. Phys. Chem.* **52** 863 (1952)
46. R A Marcus *J. Chem. Phys.* **24** 966 (1956)
47. R A Marcus *J. Chem. Phys.* **43** 679 (1965)
48. R A Marcus *J. Chem. Phys.* **43** 3477 (1965)
49. V G Levich, R R Dogonadze *Dokl. Akad. Nauk SSSR* **124** 123 (1959) [b]
50. V G Levich, R R Dogonadze *Dokl. Akad. Nauk SSSR* **133** 158 (1960) [b]
51. R R Dogonadze *Dokl. Akad. Nauk SSSR* **133** 1368 (1960) [b]
52. A A Ovchinnikov, M Ya Ovchinnikova *Zh. Eksp. Teor. Fiz.* **56** 1278 (1969) [c]
53. R R Dogonadze, A M Kuznetsov *Elektrokhimiya* **3** 1324 (1967) [d]
54. N S Hush *Electrochimica Acta* **13** 1005 (1968)
55. R A Marcus, N Sutin *Biochim. Biophys. Acta* **811** 265 (1985)
56. B Bagchi, N Gayathri *Adv. Chem. Phys.* **107** 1 (1999)
57. S V Feskov, V N Ionkin, A I Ivanov *J. Phys. Chem. A* **110** 11919 (2006)
58. R R Dogonadze, E M Itskovich, A M Kuznetsov, M A Vorotyntsev *J. Phys. Chem.* **79** 2827 (1975)
59. L Hammet *Physical Organic Chemistry. Reaction Rates, Equilibria and Mechanisms* (New York: McGraw-Hill, 1970)
60. H Leonhart, A Weller *Z. Phys. Chem. N.F.* **29** 277 (1961)
61. H Knibbe, D Rehm, A Weller *Ber. Bunsen-Ges.* **72** 257 (1968)
62. D Rehm, A Weller *Israel J. Chem.* **8** 259 (1970)
63. A Weller *Pure Appl. Chem.* **54** 1885 (1982)
64. R A Marcus, P Siders *J. Phys. Chem.* **96** 8441 (1982)
65. N Mataga, T Asahi, Y Kanda, T Okada, T Kakitani *Chem. Phys.* **127** 239 (1988)
66. I R Gould, D Ege, S L Mattes, S Farid *J. Am. Chem. Soc.* **109** 3794 (1987)
67. J R Miller, L T Calcaterra, G L Closs *J. Am. Chem. Soc.* **106** 3047 (1984)
68. K Kemnitz, N Nakashima, K Yoshihara *J. Phys. Chem.* **92** 3915 (1988)
69. P P Levin, P F Pluzhnikov, V A Kuzmin *Chem. Phys. Lett.* **147** 283 (1988)
70. I R Gould, R H Young, R E Moody, S Farid *J. Phys. Chem.* **95** 2068 (1991)
71. J R Miller *Science* **189** 221 (1975)
72. T Guarr, M McGuire, S Strauch, G McLendon *J. Am. Chem. Soc.* **105** 616 (1983)
73. J M Warman, M P de Haas, M N Paddon-Row, E Cotsaris, N S Hush, H Oevering, J W Verhoeven *Nature (London)* **320** 615 (1986)
74. D DeVault *Quantum-Mechanical Tunnelling in Biological Systems* (Cambridge: Cambridge University Press, 1984)
75. M Kumbhakar, S Nath, H Pal, A V Sapre, T Mukherjee *J. Chem. Phys.* **119** 388 (2003)
76. S J Edwards, A V Soudackov, S Hammes-Schiffer *J. Phys. Chem. B* **113** 14545 (2009)
77. A I Burshtein, A I Ivanov *Phys. Chem. Chem. Phys.* **9** 396 (2007)
78. B S Brunschwig, S Ehrenson, N Sutin *J. Am. Chem. Soc.* **106** 6858 (1984)
79. M R Wasielewski, M P Niemezyk, W A Svec, E B Pewitt *J. Am. Chem. Soc.* **107** 1080 (1985)
80. T Asahi, N Mataga, Y Takahashi, T Miyashi *Chem. Phys. Lett.* **171** 309 (1990)
81. N G Bakhshiev *Opt. Spektrosk.* **16** 821 (1964) [e]
82. V Hizhnyakov, I Tekhver *Phys. Status Solidi B* **21** 755 (1967)
83. Yu T Mazurenko, N G Bakhshiev *Opt. Spektrosk.* **28** 905 (1970) [e]
84. L D Zusman, A B Gel'man *Opt. Spektrosk.* **53** 421 (1982) [e]
85. B Bagchi, D W Oxtoby, G R Fleming *Chem. Phys.* **86** 257 (1984)
86. G Van der Zwan, J T Hynes *J. Phys. Chem.* **89** 4181 (1985)
87. R F Loring, Y J Yan, S Mukamel *J. Chem. Phys.* **87** 5840 (1987)
88. V A Mikhailova, A I Ivanov, E Vauthey *J. Chem. Phys.* **121** 6463 (2004)
89. M Cho, R J Silbey *J. Chem. Phys.* **103** 595 (1995)
90. R C Dorfman, M D Fayer *J. Chem. Phys.* **96** 7410 (1992)
91. R D Coalson, D G Evans, A Nitzan *J. Chem. Phys.* **101** 436 (1994)
92. J M Jean *J. Phys. Chem. A* **102** 7549 (1998)
93. A I Ivanov, F N Belikeev, R G Fedunov, E Vauthey *Chem. Phys. Lett.* **372** 73 (2003)
94. R G Fedunov, S V Feskov, A I Ivanov, O Nicolet, S Pagèzhs, E Vauthey *J. Chem. Phys.* **121** 3643 (2004)
95. V V Eremin, N E Kuz'menko, I M Umanskii *Khim. Fiz.* **15** 5 (1996) [f]
96. I V Rubtsov, H Shirota, K Yoshihara *J. Phys. Chem. A* **103** 1801 (1999)
97. J Cao *J. Chem. Phys.* **112** 6719 (2000)
98. J M Jean *J. Chem. Phys.* **101** 10464 (1994)
99. P F Barbara, T J Meyer, M A Ratner *J. Phys. Chem.* **100** 13148 (1996)
100. K Yoshihara, K Tominaga, Y Nagasawa *Bull. Chem. Soc. Jpn.* **68** 696 (1995)
101. K Yoshihara *Adv. Chem. Phys.* **107** 3718 (1999)
102. P J Reid, D Silva, P F Barbara, L Karki, J T Hupp *J. Phys. Chem.* **99** 2609 (1995)

103. J Najbar, R C Dorfman, M D Fayer *J. Chem. Phys.* **94** 1081 (1991)
104. P A Frantsuzov, M Tachiya *J. Chem. Phys.* **112** 4216 (2000)
105. R A Denny, B Bagchi, P F Barbara *J. Chem. Phys.* **115** 6058 (2001)
106. A Morandeira, A Furstenberg, O Nicolet, S Pagès, B Lang, E Vauthey *Chimia* **12** 690 (2002)
107. C P Koch, T Klüner, R Kosloff *J. Chem. Phys.* **116** 7983 (2002)
108. S A Kovalenko, J L P Lustres, N P Ernsting, W Rettig *J. Phys. Chem. A* **107** 10228 (2003)
109. O Nicolet, A I Ivanov, E Vauthey, in *Femtochemistry and Femtobiology: Ultrafast Events in Molecular Science* (Eds J T Hynes, M Martin) (Amsterdam: Elsevier, 2004) p. 331
110. M G Kuzmin, I V Soboleva, E V Dolotova *J. Phys. Chem.* **112** 5131 (2008)
111. A J Koch, H Meinhardt *Rev. Mod. Phys.* **66** 1481 (1994)
112. K Tominaga, D A V Kliner, A E Johnson, N E Levinger, P F Barbara *J. Chem. Phys.* **98** 1228 (1993)
113. M Seel, S Engleitner, W Zinth *Chem. Phys. Lett.* **275** 363 (1997)
114. A G Yakovlev, A Y Shkuropatov, V A Shuvalov *FEBS Lett.* **466** 209 (2000)
115. V A Shuvalov, A G Yakovlev *FEBS Lett.* **540** 26 (2003)
116. L D Zusman *Chem. Phys.* **49** 295 (1980)
117. P F Barbara, W Jarzeba *Adv. Photochem.* **15** 1 (1990)
118. J D Simon, R Doolen *J. Am. Chem. Soc.* **114** 861 (1992)
119. F Poellinger, H Heitele, M E Michel-Beyerle, C Anders, M Futscher, H A Staabet *Chem. Phys. Lett.* **198** 645 (1992)
120. K Wynne, R Hochstrasser *Adv. Chem. Phys.* **107** 263 (1999)
121. S K Doorn, P O Stoutland, R B Dyer, W H Woodruff *J. Am. Chem. Soc.* **114** 3133 (1992)
122. M H Vos, F Rappaport, J-C Lambry, J Breton, J-L Martin *Nature (London)* **363** 320 (1993)
123. J Zhou, B R Findley, C L Braun, N Sutin *J. Chem. Phys.* **114** 10448 (2001)
124. A I Ivanov, V V Potovoi *Opt. Spektrosk.* **86** 755 (1999) [e]
125. A I Ivanov, A V Kuchin *Zh. Fiz. Khim.* **73** 2170 (1999) [g]
126. G Grampp, A I Ivanov, A V Kuchin *Zh. Fiz. Khim.* **75** 2242 (2001) [g]
127. A I Ivanov *Chem. Phys. Lett.* **229** 671 (1994)
128. A I Ivanov, V A Mikhailova, S V Fes'kov *Zh. Fiz. Khim.* **71** 1500 (1997) [g]
129. K Ando, H Sumi *J. Chem. Phys.* **102** 10991 (1998)
130. A I Ivanov, V A Mikhailova *Zh. Fiz. Khim.* **80** 1053 (2006) [g]
131. A I Ivanov, V N Ionkin, S V Fes'kov *Zh. Fiz. Khim.* **82** 374 (2008) [g]
132. S V Feskov, V N Ionkin, A I Ivanov, H Hagemann, E Vauthey *J. Phys. Chem. A* **112** 594 (2008)
133. A I Shushin *Chem. Phys.* **60** 149 (1981)
134. N Mataga, H Miyasaka *Adv. Chem. Phys.* **107** 431 (1999)
135. T Elsaesser, W Kaiser *Annu. Rev. Phys. Chem.* **42** 83 (1991)
136. S A Kovalenko, R Schanz, H Hennig, N P Ernsting *J. Chem. Phys.* **115** 3256 (2001)
137. V A Mikhailova, A I Ivanov *J. Phys. Chem. C* **111** 4445 (2007)
138. A I Ivanov, V A Mikhailova *Khim. Fiz.* **27** (9) 5 (2008) [f]
139. R R Dogonadze, A M Kuznetsov, in *Kinetika Khimicheskikh Reaktsii v Polyarnykh Rastvoritelyakh (Itogi Nauki i Tekhniki. Fizicheskaya Khimiya. Kinetika)* [Kinetics of Chemical Reactions in Polar Solvents (Advances in Science and Engineering. Physical Chemistry. Kinetics)] (Moscow: Izd. VINITI, 1973) Vol. 2, p. 215
140. J Jortner, M Bixon *J. Chem. Phys.* **88** 167 (1988)
141. D V Dodin, A I Ivanov *Chem. Phys.* **303** 63 (2004)
142. S Garg, C Smyth *J. Phys. Chem.* **69** 1294 (1965)
143. R Jimenez, G R Fleming, P V Kumar, M Maroncelli *Nature (London)* **369** 471 (1994)
144. P J Reid, P F Barbara *J. Phys. Chem.* **99** 3554 (1995)
145. H Risken, in *The Fokker – Planck Equation* (Berlin: Springer, 1989) p. 485
146. B I Yakobson, A I Burshtein *Chem. Phys.* **49** 385 (1980)
147. V Gladkikh, A I Burshtein, S V Feskov, A I Ivanov, E Vauthey *J. Chem. Phys.* **123** 244510 (2005)
148. O Nicolet, N Banerji, S Pages, E Vauthey *J. Phys. Chem. A* **109** 8236 (2005)
149. V N Ionkin, A I Ivanov *Chem. Phys.* **360** 137 (2009)
150. R G Fedunov, A I Ivanov *J. Chem. Phys.* **122** 064501 (2005)
151. S S Khohlova, V A Mikhailova, A I Ivanov *J. Chem. Phys.* **124** 114507 (2006)
152. A I Ivanov, V A Mikhailova, S S Khokhlova *Zh. Fiz. Khim.* **80** 1702 (2006) [g]
153. S S Khokhlova, V A Mikhailova, A I Ivanov *Khim. Fiz.* **26** (7) 27 (2007) [f]
154. S S Khokhlova, V A Mikhailova, A I Ivanov *Zh. Fiz. Khim.* **82** 1161 (2008) [g]
155. A Osuka, T Nagata, F Kobayashi, R P Zhang, K Maruyama, N Mataga, T Asahi, T Ohno, K Nozaki *Chem. Phys. Lett.* **199** 302 (1992)
156. D G Johnson, M P Niemczyk, D W Minsek, G P Wiederrecht, W A Svec, G L Gaines, M R Wasielewski *J. Am. Chem. Soc.* **115** 5695 (1993)
157. A M Brouwer, C Eijckelhoff, R J Willemse, J W Verhoeven, W Schuddeboom, J M Warman *J. Am. Chem. Soc.* **115** 2988 (1993)
158. S -C Hung, A N Macpherson, S Lin, P A Liddell, G R Seely, A L Moore, T A Moore, D Gust *J. Am. Chem. Soc.* **117** 1657 (1995)
159. A Harriman, F Odobel, J-P Sauvage *J. Am. Chem. Soc.* **116** 5481 (1994)
160. B Boldrini, E Cavalli, A Painelli, F Terenziani *J. Phys. Chem.* **106** 6286 (2002)
161. E Vauthey *Chem. Phys. Lett.* **216** 530 (1993)
162. E W Castner, J D Kennedy, R J Cave *J. Phys. Chem.* **104** 2869 (2000)
163. J Najbar, M Tachiya *J. Phys. Chem.* **98** 199 (1994)
164. T Motylewski, J Najbar, M Tachiya *Chem. Phys.* **212** 193 (1996)
165. N Mataga, Y Kaifu, M Koizumi *Bull. Chem. Soc. Jpn.* **28** 690 (1955)
166. E Lippert *Z. Naturforsch. A* **10** 541 (1955)
167. L Onsager *J. Phys. Chem.* **43** 189 (1939)
168. E Lippert *Z. Electrochem.* **61** 962 (1957)
169. F E Gostev, A E Dzhailaubekov, A N Petrukhin, A A Titov, S Ya Umanskii, O M Sarkisov *Khim. Fiz.* **19** (12) 11 (2000) [f]
170. O M Sarkisov, A N Petrukhin, F E Gostev, A A Titov *Kvantovaya Elektronika* **31** 483 (2001) [*Quant. Electron.* **31** 483 (2001)]
171. J Zhou, B R Findley, A Teslja, C L Braun, N Sutin *J. Phys. Chem. A* **104** 11512 (2000)
172. M F Gelin, D Egorova, W Domcke *J. Chem. Phys.* **131** 124505 (2009)
173. S A Kovalenko, A L Dobryakov, V Farztdinov *Phys. Rev. Lett.* **96** 068301 (2006)
174. A I Ivanov, R G Fedunov, S V Fes'kov *Zh. Fiz. Khim.* **78** 1448 (2004) [g]
175. V N Ionkin, A I Ivanov, E Vauthey *Zh. Fiz. Khim.* **83** 791 (2009) [g]
176. H Chosrowjan, S Tanigichi, T Okada, S Takagi, T Arai, K Tokumaru *Chem. Phys. Lett.* **242** 644 (1995)
177. N Mataga, Y Shibata, H Chosrowjan, N Yoshida, A Osuka *J. Phys. Chem. B* **104** 4001 (2000)
178. N Mataga, H Chosrowjan, Y Shibata, N Yoshida, A Osuka, T Kikuzawa, T Okada *J. Am. Chem. Soc.* **123** 12422 (2001)
179. N Mataga, H Chosrowjan, S Taniguchi, Y Shibata, N Yoshida, A Osuka, T Kikuzawa, T Okada *J. Phys. Chem. A* **106** 12191 (2002)
180. A Morandeira, L Engeli, E Vauthey *J. Phys. Chem. A* **106** 4833 (2002)
181. S Wallin, C Monnereau, E Blart, J-R Gankou, F Odobel, L Hammarström *J. Phys. Chem. A* **114** 1709 (2010)
182. N Mataga, S Taniguchi, H Chosrowjan, A Osuka, N Yoshida *Chem. Phys.* **295** 215 (2003)
183. N Mataga, H Chosrowjan, S Taniguchi *J. Photochem. Photobiol. C* **6** 37 (2005)
184. V N Ionkin, A I Ivanov *J. Phys. Chem. A* **113** 103 (2009)

185. M L Horng, J A Gardecki, A Papazyan, M Maroncelli *J. Phys. Chem.* **99** 17311 (1995)
186. S V Feskov, A I Burshtein *J. Phys. Chem. A* **113** 13528 (2009)
187. H Torieda, K Nozaki, A Yoshimura, T Ohno *J. Phys. Chem. A* **108** 4819 (2004)

[a] — *Nanotechnol. Russ. (Engl. Transl.)*
[b] — *Dokl. Phys. (Engl. Transl.)*
[c] — *J. Exp. Theor. Phys. (Engl. Transl.)*
[d] — *Russ. J. Electrochem. (Engl. Transl.)*
[e] — *Opt. Spectrosc. (Engl. Transl.)*
[f] — *Russ. J. Phys. Chem., Ser. B (Engl. Transl.)*
[g] — *Russ. J. Phys. Chem., Ser. A (Engl. Transl.)*